

High-Level Teleoperation System For Aerial Exploration Of Indoor Environments

W. Alexander Isop^{1*}, Christoph Gebhardt², Tobias Nägeli²,
Friedrich Fraundorfer¹, Otmar Hilliges², Dieter Schmalstieg^{1,3}

¹Institute of Computer Graphics and Vision, Department of Computer Science, Graz University of Technology, 8010 Graz, Austria

²AIT Lab, Department of Computer Science, ETH Zürich, Zurich 8092, Switzerland

³VRVis Research Center, 1220 Vienna, Austria

Correspondence*:
W. Alexander Isop
isop@icg.tugraz.at

2 **Number of Words:** 11483, **Number of Figures:** 11

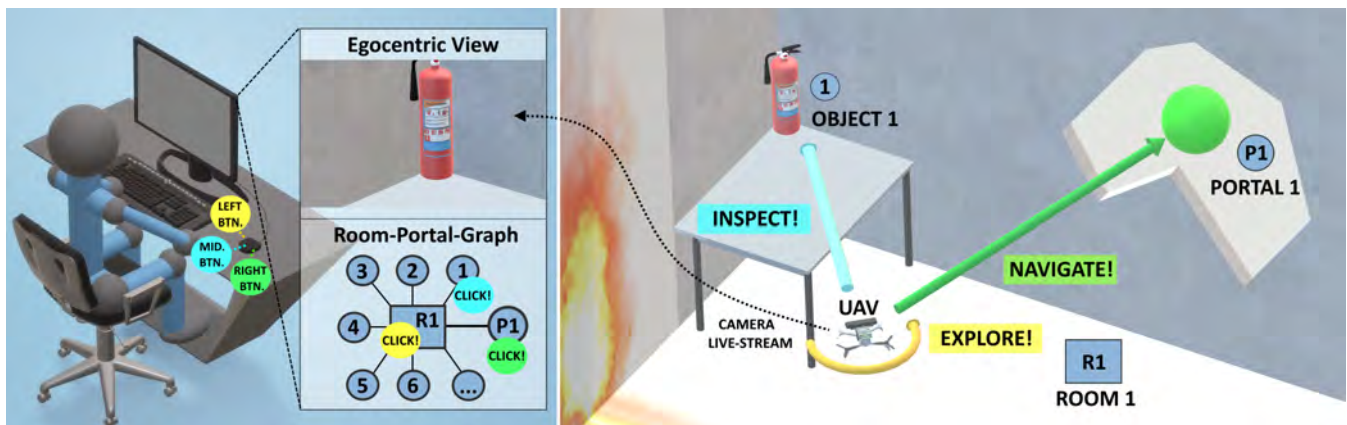


Figure 1. High-Level teleoperation system. (left) The room-portal graph displays an interactive topological view of an indoor environment, created in real-time, to facilitate automation. (right) Conceptual illustration of the aerial telerobot, implemented as unmanned aerial vehicle (UAV), and its according high-level tasks.

3 **ABSTRACT**

4 Exploration of challenging indoor environments is a demanding task. While automation with
5 aerial robots seems a promising solution, fully autonomous systems still struggle with high-level
6 cognitive tasks and intuitive decision making. To facilitate automation, we introduce a novel
7 teleoperation system with an aerial telerobot that is capable of handling all demanding low-
8 level tasks. Motivated by the typical structure of indoor environments, the system creates an
9 interactive scene topology in real-time that reduces scene details and supports affordances. Thus,
10 difficult high-level tasks can be effectively supervised by a human operator. To elaborate on the
11 effectiveness of our system during a real-world exploration mission, we conducted a user study.
12 Despite being limited by real-world constraints, results indicate that our system better supports
13 operators with indoor exploration, compared to a baseline system with traditional joystick control.

14 **Keywords:** teleoperation system, telerobotics, system design, scene abstraction, unmanned aerial vehicles, indoor exploration

1 INTRODUCTION

15 Teleoperation of small-sized aerial robots in indoor environments is important for applications like search-
16 and-rescue or exploration missions. A recurring problem in such applications is lack of situation awareness
17 and consequently decreasing overall task performance (Stubbs et al., 2007; Burke and Murphy, 2004).

18 One important aspect is that with an increasing amount of scene details, operators struggle to comprehend
19 the visualized information of the teleoperation system (Atherton and Goodrich, 2009). While it is required
20 that the system presents the information in a way that does not overwhelm the operator, also the levels
21 of autonomy (LOA) play a crucial role. Increasing autonomy of the system can improve operators task
22 performance by reducing their mental load. The goal is to free up the operators to be engaged in other
23 important high-level tasks (Goodrich et al., 2007), such as navigation or identification of victims or
24 hazards. However, related work has shown that true full autonomy is still hard to accomplish for complex
25 missions (MahmoudZadeh et al., 2018). This emphasizes difficulty of an optimal level of autonomy for a
26 teleoperation system. As a tradeoff, approaches were introduced in which operators can explicitly adjust the
27 autonomy of the system to the desired level (Bruemmer et al., 2002; Muszynski et al., 2012). Unfortunately,
28 such approaches typically consider a handover to low-level demanding tasks (Reese, 2016). While trading
29 off task automation and manual control is task-specific and remains non-trivial to date, our system on
30 one hand suggests to automate all low-level tasks. On the other hand, high-level tasks can be accessed
31 via an interactive scene with reduced details. Yet, the question remains how such a system effects aerial
32 exploration missions in a real-world setting.

33 To investigate this question, we introduce a fully working teleoperation system. The system uses a small-
34 sized aerial telerobot to perform the challenging task of indoor exploration. In particular, our system is
35 capable of: i) indoor navigation in the presence of narrow spaces and wind-turbulence without collision;
36 ii) automated repetitive exploration and navigation of structured spaces; iii) detection and navigation of
37 constrained spaces, like narrow gateways or windows, without collision; iv) and detection of objects of
38 interest (OOIs), like victims or fire extinguishers. To relieve the operator, the system automates all low-level
39 mission-critical tasks (see Figure 5). However, we allow the operator to override non-mission-critical,
40 high-level objectives. This results in a design where the system usually runs at the highest LOA (*highest*
41 *automation*), but can be effectively supervised at collaborative level (*high automation*) if necessary (see
42 Table 2)¹.

43 The operator supervises the teleoperation system using a multi-view GUI which consists of a traditional
44 egocentric scene view, an exocentric scene view, and a complementary topological graph view of the scene,
45 called the room-portal graph (RPG) (see Figure 2). The RPG represents the scene as a subdivision of rooms
46 connected by portals, creating a clearly distinguishable spatial structure of a typical indoor environment.
47 The RPG reduces scene details and allows fast comprehension of important scene structure and objects
48 during an exploration mission. It is interactive and lets the operator improve time-performance and resolve
49 system failures, for example false detection of OOIs.

50 To understand the task effectiveness of our teleoperation system in a real-world setting, we conducted a user
51 study. Participants accomplished an exploration mission using our proposed system and, in comparison,
52 using a baseline system with traditional joystick control. While results indicate increased task performance
53 and comfort with the outcome of our experiments, our findings provide evidence that our system can better
54 support operators with challenging aerial indoor exploration missions.

¹ The reported levels of automation (LOA) are based on the ALFUS framework of Huang et al. (2005a,b).

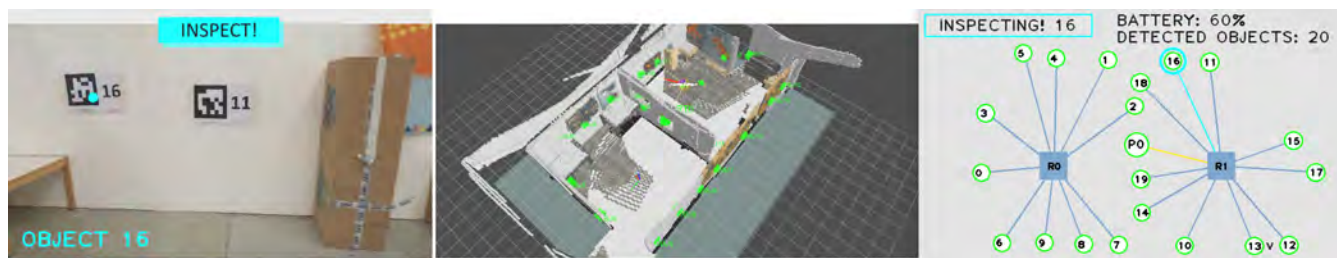


Figure 2. Implementation of the RPG as part of our high-level teleoperation system. It is presented during an inspection task, after full exploration of two connected rooms. (left) Egocentric virtual live view from the on-board camera of the UAV, highlighting an inspected object. (middle) Exocentric virtual 3D view of the reconstructed scene. (right) Interactive, topological RPG of the same scene, with two rooms (represented as squares), detected objects including a portal. Objects are shown as round labels with leader lines. Inspected objects are highlighted.

55 In summary, we contribute: i) a fully working teleoperation system for aerial indoor exploration missions,
 56 including a real-time interactive scene topology that enables supervisory control of high-level tasks,
 57 and ii) the empirical evidence that such a system effectively supports human operators during realistic
 58 exploration missions. In the remainder of the paper, we provide an extensive overview on related work,
 59 including a brief history of teleoperation and current state-of-the-art systems. We present details of design
 60 rationals and implementation of our system, as well as limitations. Followed by reporting on experimental
 61 design and results of our user study, we finally conclude our paper and propose interesting directions for
 62 future work.

2 RELATED WORK

63 The research conducted in the area of robotic teleoperation is extensive and was explored starting from the
 64 mid of the 20th century. The research is highly interdisciplinary and addresses a rich variety of aspects
 65 in human-robot-interaction, mobile robotics and visualization. The purpose of this section is to help the
 66 reader to understand the complexity of the field and to provide an overview of state-of-the-art systems. It
 67 starts with a short historical summary of teleoperation. It continues with a broad range of related work
 68 regarding telerobotics and ends with addressing specific work on high-level indoor exploration with aerial
 69 teleoperation systems. Thus, we provide an extensive literature survey and discussion about origin and
 70 history of robotic teleoperation, its motivation, typical use cases and changing demands to the system
 71 over time. Finally, it adds a discussion about limitations and potential future work to relevant sections.
 72 Ultimately, our goal is to help the reader to better understand the motivation of our system and its novelty
 73 in the presented form.

74 2.1 History Of Teleoperation - From The Poking Of Fire To Telerobotics in Space

75 Interestingly, an extensive survey by Lichiardopol (2007) suggests that the first form of teleoperation was
 76 the poking of fire in the early age of human mankind. By utilizing the stick to set fire, the human was
 77 actually teleoperating (or telemanipulating) the fire place. A million years later, in the early 1900's, for
 78 the first time teleoperation appeared for piloting unmanned aircrafts (Fong and Thorpe, 2001). Related
 79 work continues in the mid of the past century, but in the context of remote handling hazardous materials.
 80 According to an extensive summary of Vertut and Coiffet (1986), R. Goertz worked on a pantograph as
 81 telemanipulation device for radioactive materials inside a nuclear reactor. The obvious purpose was to
 82 enable safe handling of the otherwise dangerous materials by human operators. In the following decades,

83 the need for robotic teleoperation significantly increased, also highlighted as part of a comprehensive survey
84 of Alexander (1972). In his work, Alexander (1972) declares the terms teloperation and telemanipulation
85 under "telemation" and investigates on which use cases in the civil sector development on teleoperation
86 systems would have greatest impact. Amongst nuclear reactor fuel handling, mining, oceanographic and
87 medical teleoperation systems, additionally a strong need for teleoperation was growing in aeronautics and
88 space (Corliss and Johnson (1967), Alexander III (1973)). At this point, the original purpose of robotic
89 teleoperation becomes apparent, which is to enable a human operator to work at a (larger) distance in
90 hazardous environments. According to Lichiardopol (2007), this requires the following essential definitions:

- 91 •**(autonomous) Teleoperator:** The automatically operated machine that replaces human effort, though it
92 may not resemble human beings in appearance or perform functions in a humanlike manner.
- 93 •**Operator:** A human operator is the person who monitors the operated machine and takes control of the
94 required actions.
- 95 •**Teleoperation:** The task or activity itself to "operate a vehicle or a system over a distance" (Fong and
96 Thorpe, 2001).

97 More recent work about teleoperation (Cui et al., 2003) gives a clearer overview of the required main
98 components, data-flow and interfaces. These are in particular:

- 99 •**Remote System (teleoperator or telerobot):** which is a machine or robot that enables a human operator
100 to move about, sense and mechanically manipulate objects at a distance.
- 101 •**Human Machine Interface (human-robot interface):** A software framework, including a graphical user
102 interface (GUI) software, control software and interface software to process sensory data.
- 103 •**Manual Control Unit (input device):** Including an input device for manual control inputs.

104 By definition, the human operator manually interacts with the teleoperation system via the input device,
105 whereas the telerobot senses and performs actions in the far distant environment.

106 2.2 Telerobots - Reducing Human Effort

107 According to Cui et al. (2003), telerobots are a subclass of teleoperators. They are typically implemented
108 as mobile robots that accept instructions from a human operator at a distance. Moreover, they perform
109 live actions at a distant environment through the use of sensors or other control mechanisms. Usually
110 they have sensors and/or effectors for manipulation and/or mobility, and moreover provide mechanisms
111 for the human operator to communicate with both. Due to the rich variety of applications and remote
112 environments, related work addressed various types and sizes of mobile robots during the past decades.
113 Such are ranging from space exploration-, mining-, medical- and underwater-applications (Alexander III
114 (1972), Sheridan and Verplank (1978)) in the early years of modern teleoperation, to humanoid telepresence
115 robots with increasing popularity in the early 2000s (Lichiardopol, 2007) and more recent telerobots for
116 bomb defusal (Technology, 2014). Amongst others, important types of telerobots include stationary robots
117 like arm manipulators (Murray (2017), Rakita et al. (2018)), underwater robots (Costa et al., 2018), ground
118 based search and rescue robots (Stepanova et al., 2017), humanoid robots for telepresence (Cortellessa
119 et al., 2018) and aerial telerobots for surveillance (Jha, 2016) or exploration and mapping (Papachristos
120 et al., 2017).

121 In particular, small sized UAVs or micro aerial vehicles (MAVs) soared popularity in the past decades (Cai
122 et al., 2014). While their small size and low weight make them attractive for research and education (Wu
123 et al., 2018), they are also extensively used outdoors for industrial purposes. Typical use cases involve

124 agriculture (Tripicchio et al., 2015), medical transportation (Scalea et al., 2019) and moreover search and
125 rescue or exploration missions (Silvagni et al., 2019). However, such use cases put different demands
126 on the UAV, compared to indoor flights. In outdoor environments spatial constraints play a subsidiary
127 role and very often GPS-based localization and navigation is possible. In contrast, exploration of indoor
128 environments requires small UAV dimensions to avoid problems with reaching narrow passages. Also,
129 typical limitations remain like onboard computational power and flight times. Furthermore, low-thrust
130 propulsion is important, since turbulences could strongly affect stability and overall flight performance
131 of the UAV. State of the art off-the-shelf UAVs which could be potentially used for such purposes are
132 the DJI Mavic or the Intel Aero platform. However, on one hand, such solutions are more bulky and
133 heavy and are not easily customizable (software interfaces, sensors). On the other hand, smaller and
134 more lightweight solutions (Kushleyev et al. (2013); Loiano et al. (2016)) are more limited regarding
135 payload and flight times. Very recent UAV designs with similar all-up-weight and dimensions (Sanket
136 et al. (2018); Falanga et al. (2019)) also discuss navigation and exploration of portals. Though, they either
137 provide shorter hover flight times or do not carry Kinect-like RGB-D sensors. Such are used for creating
138 dense mapping data (Henry et al., 2012), while this can be beneficial for indoor exploration. In general,
139 to achieve an optimal UAV design for aerial exploration and online mapping of indoor environments still
140 remains difficult. A potential future design, also reflecting the room for improvement of our presented UAV,
141 may include the following challenging specifications if combined in one system:

- 142 • **Small-scale dimension** with tip-to-tip diameter under $100mm$ (Giernacki et al., 2017) (approx. size of
143 the palm of a humans hand) which would enable it to reach very narrow passages and make it easy to
144 hold and carry.
- 145 • **Low all-up-weight** below $100g$ (Kushleyev et al., 2013) to make transportation easier and reduce
146 produced thrust and turbulences during flight.
- 147 • **Low-weight sensors** including kinect-like or omnidirectional vision sensors.
- 148 • **Powerful computing units** (e.g. Tegra K1, Kyristis et al. (2016)), including GPUs to execute all tasks
149 which are important for exploration of indoor environments onboard (robust localization, exploration,
150 navigation, motion planning, online mapping and object recognition).
- 151 • **Increased flight times** of more than $30mins$, which is typical for state of the art commercial UAVs
152 in this size- and weight-category (Robotics, 2019), or extendable flight times by autonomous wireless
153 recharging technology (Junaid et al. (2016), Al-Obaidi et al. (2019)).

154 2.3 Remote Connection - Coping With The Issues Of Time Delay

155 Although the remote connection between telerobot and human-robot interface is not listed as an individual
156 component by Cui et al. (2003), it has major impact on the overall task performance. According to a survey
157 of Sheridan (1993), time delay is a "serious problem for teleoperation". Issues with time delays were
158 for the first time addressed in the early 1960's by (Adams, 1961), whereas later work by Ferrell (1965)
159 found that human operators can cope with time delays by using a simple "move and wait strategy". His
160 experiments also showed that task performance is linearly dependent and predictable on the time-delay
161 during teleoperation. Remarkably, Held et al. (1966) found that sensory-motor adaptation is essentially
162 impossible for delays as small as $0.3s$, and that human operators dissociate the teleoperator movements
163 from those of their own in the presence of such delays (Held and Durlach, 1991). Especially if direct control
164 methods are used, this could lead to a nonoptimal task performance and Sheridan (1992) explicitly states
165 that direct control in the presence of delay (transmission or otherwise) is tedious, fatiguing, and error prone.
166 Since our teleoperation system includes a wireless remote connection with potential higher time-delays

167 ($> 0.3s$), this also affected our design decisions about the control approach (Section 3.2.1). More recent
168 related work discusses impact of time delays during teleoperation of small-sized UAVs (Riestock et al.,
169 2017a,b), whereas they elaborate on effects of limited bandwidth on the GUI. They compare operators
170 performance during collision avoidance tasks and use traditional egocentric live camera views and grid-map
171 representations of the scene. Interestingly, their results indicate that the operator performance suffered less
172 under a change of communication quality using grid-maps, compared to the egocentric live camera views.
173 Consequently this was considered in the design of our GUI (Section 3.2.2).

174 2.4 Human-Robot Interfaces - Facilitating Control And Cognition

175 Based on the summary of Cui et al. (2003), the human-robot interface processes data of sensors and
176 actuators of the telerobot for control, typically at different LOA. It further visualizes information about
177 the remote system and the remote scene with a GUI. Finally, it is responsible for processing the operators
178 manual inputs of the input device.

179 2.4.1 Levels of Automation And Approaches For Control

180 The LOA of a teleoperation system is important, since it could have great impact on the overall design
181 of the teloperation system (Save et al. (2012), Endsley (2018)). Moreover, the LOA greatly effects the
182 operators overall task performance during teleoperation (Materna et al., 2017). Subsequently, also a variety
183 of taxonomies for LOA were introduced for robotic teleoperation. While the idea of LOA was introduced
184 by(Sheridan and Verplank, 1978) in the late 1970s for underwater teleoperation applications, more recent
185 work broadened this concept (Endsley, 1999; Parasuraman et al., 2000). Depending on the application,
186 related work discusses various models with more or less fine grained LOA for flight traffic control (Council
187 et al., 1998), manufacturing (Frohm et al., 2008) and, most recently, autonomous driving (SAE, 2014).
188 Most interesting four our work is a LOA-taxonomy specifically designed for unmanned systems. Introduced
189 by Huang et al. (2005b,a), it was successfully adapted for indoor exploration missions by Valero-Gomez
190 et al. (2011).

191 On one hand, low LOA typically imply that the human operator has direct *manual control* over the telerobot
192 and can also directly access detailed sensory data (Sheridan, 1992). However, the operator must be also able
193 to process and interpret this data. During challenging tasks under time constraints, this could overwhelm
194 the operator and lead to decreased task performance or even mission failure. On the other hand, so called
195 "fully automated systems" without any control of an operator are still hard to put into practice. At least their
196 overall performance can be still significantly improved if they are teamed with a human (Johnson and Vera,
197 2019). In order, also the design of our human-robot interface is motivated by the capabilities and moreover
198 limitations of the telerobot. The presented GUI builds on top, enabling the human to supervise with difficult
199 high-level tasks. Automation at higher levels means that the telerobot is able to accomplish certain low-level
200 tasks independently and could relieve the operator based on *supervisory control* (Sheridan, 1992). If the
201 telerobot fails, on demand switching the system to lower LOA could be helpful (*adjustable or sliding*
202 *autonomy*), whereas an extensive survey is presented by (Mostafa et al., 2019). Muszynski et al. (2012),
203 Bruemmer et al. (2005), Chen et al. (2013) and Leeper et al. (2012) propose teleoperation systems with
204 different LOA for control of ground-based robots from classical egocentric and exocentric views. These
205 works consistently report on improved operator performance with increasing autonomy. Extensive research
206 has been conducted concerning the concept of switching between LOA. Valero-Gomez et al. (2011) suggest
207 two autonomy models to interact with robot teams during exploration missions and enable low-level
208 operation on demand. Fong et al. (2003) explored semi-autonomous systems that query users for input, in
209 case of uncertain decision. Both papers suggest that system failures should be handled manually by the

operator. However, their design focuses on ground based navigation or grasping. They also do not provide a minimum LOA to the operator, avoiding mission-critical tasks during flight missions. To cope with the issues of direct control, Gebhardt et al. (2016), Nægeli et al. (2017b) and Nægeli et al. (2017a) suggest optimized planning of constrained quadrotor paths. They also avoid passing low-level tasks to the operator and instead introduce indirect, high-level flight goals. They allow inexperienced operators to control the UAV without deeper knowledge of the underlying methods for quadrotor control or the target domain. An important prerequisite for such ease of use is that the UAV can move along a collision-free path. More recent work combining supervisory control and adjustable autonomy is presented by Lin and Goodrich (2015), Szafer et al. (2017) and Lan et al. (2017). Remarkable limitations with all supervisory control approaches are the *lumberjack effect* (Onnasch et al., 2014) and the *automation conundrum* (Endsley, 2017). These effects summarize a tradeoff between high LOA improving task performance and problems with sudden passing of low-level tasks if problems occur. Moreover, a general concept that provides an optimum LOA and level of operator control for all applications and tasks seems impossible and will remain difficult in the future. Such limitations must be considered in the design of the teleoperation system. Consequently, also our system avoids sudden passing of low-level functions to the operator and only allows for overriding functions at high LOA (supervisory control). In contrast to related work, the LOA design of our work considers challenging tasks that occur during aerial indoor exploration missions. Design details can be found in Section 3.2.

2.4.2 Graphical User Interfaces

Various types of GUIs, with different combination of scene views, have been investigated to improve task efficiency for teleoperation of small-sized UAVs. Examples range from interfaces with traditional egocentric live camera views (Cho et al., 2017), combined with direct joystick based control, to fully immersive interfaces utilizing the operators upper body for control (Rognon et al., 2018).

As an alternative to UAV navigation from egocentric views, direct commands can be issued in an adaptive exocentric perspective (Saakes et al., 2013; Thomason et al., 2017, 2019) or from a 3D map view (Materna et al., 2017). The exocentric view can improve the operator's understanding of the environment and further increase safety and task performance. Additionally, concepts of switching between ego- and exocentric views is discussed by Baudisch et al. (2002) whereas Ferland et al. (2009) suggest to switch between egocentric and exocentric views for robot teleoperation. Following the overview- and detail paradigm, their overall goal is to improve task performance by providing information details on demand. According to Gebhardt et al. (2016) and Nægeli et al. (2017a), pure exocentric planning views can be beneficial for applications such as robotic light painting, drone-racing and aerial cinematography. Also the work of Lan et al. (2017) combines exocentric scene views with a high-level GUI for photo taking with a semi-autonomous UAV. However, these applications do not generate an interactive scene topology from 3D data. They either require that a 3D map is already pre-generated or use mapping for localization and path planning only. Importantly, they do not consider challenging tasks that occur during indoor exploration missions, like flight through narrow passages. In contrast, the design of our system focuses on flight missions in challenging indoor environments. Most importantly, we generate an interactive scene topology in real-time and thus facilitate automation.

Remarkably, only providing exocentric 3D map views can lead to problems. For example, Chellali and Baizid (2011) state that on one hand the third dimension is an additional degree of freedom that helps to add constraints and information to disambiguate location of objects. On the other hand, they report on significantly decreased task performance when localizing objects in 3D maps, compared to localization in 2D. They suggest that the additional dimension provided within 3D maps leads to a greater space to

254 explore and thus the operator needs more time. This tradeoff was also considered in the design of our GUI,
255 which is outlined in Section 3.2.2.

256 By even more reducing scene details, abstract topological views prevent the operator from being
257 overwhelmed and typically rely on 2D or 3D data (Richtsfeld et al., 2012; Yang and Worboys, 2015;
258 Wang et al., 2018). Bormann et al. (2016) and Ambrus et al. (2017) introduce segmentation of rooms
259 in indoor environments. The goal of their work is to provide the segmented data to mobile robots for
260 autonomous navigation. In contrast, Kortenkamp (1993), Choset and Nagatani (2001), Schröter et al.
261 (2003), Vasudevan et al. (2007) and Angeli et al. (2008) represent the environmental understanding of a
262 mobile robot in a way that facilitates human comprehension. They suggest a topological representation
263 of places visualized as object graphs. The visualization of the environment is hierarchical, and strongly
264 motivates usage for navigation. However, highlighting OOIs in real-time during flight missions is not
265 investigated. Yang and Worboys (2015) also supports structuring of indoor spaces into rooms and portals
266 from offline generated data. Kun et al. (2017) report on an ontology-based navigation model as part of
267 an indoor positioning framework, introducing basic categories of abstract 2D objects (right Figure 3).
268 All these approaches strongly support design of an abstract comprehensive representation of the scene to
269 compute interactive navigation graphs for an indoor space (Section 3.2.2). However, none of these authors
270 evaluate real-time generation of an interactive scene topology as part of a teleoperation system for aerial
271 indoor exploration under real-world constraints.

272 **2.5 Input Devices - Enabling Manual Control**

273 Extensive research on teleoperation of small sized aerial robots with various types of input-devices and
274 according interactions, has been conducted in the past decade. Despite the popularity of novel interaction
275 paradigms, like hand-gesture (Yu et al., 2017; Duan et al., 2018), body-gesture (Rognon et al., 2018),
276 gaze (Yu et al., 2014; Erat et al., 2018; Yuan et al., 2019) and language (Huang et al., 2010, 2019)), more
277 recent work still focuses on aspects of traditional joystick based teleoperation of small-sized UAVs, for
278 example avoiding collisions during navigation (Cho et al., 2017). Interestingly, Sanders et al. (2018) report
279 that operators still prefer joystick control over indirect gaze based steering, whereas findings of Herrmann
280 and Schmidt (2018) indicate that a traditional input device is more efficient than their extensive and
281 carefully designed system based on natural interactions. In conclusion, if task-efficiency is preferred over
282 user experience (fun to use, increasing enjoyment during teleoperation) traditional input devices are still
283 hard to outperform. Remarkably, joystick controls can be still considered as state-of-the-art input device
284 and are commonly chosen as baseline for performance evaluations. As a consequence, also our work aimed
285 for selecting a traditional input device and according interaction design which would be able to compete
286 against conventional joystick controls. Experimental results are detailed in Section 6.1. Other important
287 aspects were required pre-training, complexity and cost-effectiveness. Details of the according design
288 rationales can be found in Section 3.3.

289 **2.6 High-Level Teleoperation Systems For Exploration Of Indoor Environments**

290 Very recent work on fully working teleoperation systems for indoor environments is for example discussed
291 by Valner et al. (2018). In their work they introduce high-level interaction methods based on gesture and
292 language, but for ground-based robots. While they also suggest seamless switching between navigation,
293 inspection and manipulation tasks, they use traditional egocentric 2D views and a 3D map to improve task
294 performance. Recent work on fully working teleoperation systems, but with aerial telerobots is discussed
295 by Hedayati et al. (2018), Walker et al. (2019), Huang et al. (2019) and Paterson et al. (2019). All systems
296 use state-of-the-art AR, MR or VR input devices, whereas they also design high-level interactions for their



Figure 3. Example map views of complex office environments with gradual loss of details. left) Full 3D map view. middle) Floorplan in 2D. right) Topological view (Kun et al., 2017).

297 human-robot interface. Their overall goal is to improve task-efficiency when commanding aerial telerobots
 298 in indoor environments. Remarkably, they all compare their teleoperation systems against baseline systems
 299 (using traditional joystick or keyboard controls) and their independent variable in the study corresponds to
 300 what type of teleoperation interface the participants used. Though, their systems are based on natural gaze
 301 or language commands and do not refer to an interactive 2D scene topology created in real-time. Further,
 302 they do not consider aerial exploration missions in challenging indoor environments where simple and
 303 robust input devices can be beneficial to improve task performance. Related work, which might be closest
 304 to ours, is presented by Szafir et al. (2017). The work presents three prototypes with different methods
 305 to control an aerial telerobot. Interestingly, they also make use of an abstract floor-plan representation of
 306 the scene. However, this plan is static and not autonomously created in real-time. Although related work
 307 already proposed abstract topological views for the control of teleoperation systems, to our understanding
 308 we are the first who introduce a fully working system that refers to an interactive scene topology, created in
 309 real-time during flight. This raises the interesting question, if the performance of our teleoperation system
 310 is also preserved when put into practice. Compared to a variety of related teleoperation systems with similar
 311 mission complexity (Cho et al., 2017; Riestock et al., 2017b; Thomason et al., 2017), we evaluate the
 312 performance of our fully working system with a user study under real-world constraints (Section 6.1).

3 SYSTEM DESIGN RATIONALES

313 The design of our teleoperation system is highly task-oriented for the purpose of aerial exploration. It
 314 focuses on exploration of civil buildings with constrained indoor spaces and repeating room geometry.
 315 Example representations of an office building are shown in left and middle Figure 3 (3D map and 2D
 316 floorplan). Typically, an exploration mission would require to navigate inside the building and detect
 317 OOIs (fire extinguishers or trapped victims). For such applications teleoperation systems can be helpful,
 318 if disaster relief forces are not able to reach inside such buildings and assessment of the situation is
 319 required (Lichiardopol, 2007). In order, our teleoperation system uses the same main components as
 320 state-of-the-art systems (Figure 4):

- 321 •Aerial Telerobot: Our telerobot is a small-sized UAV, holding various sensors (cameras and inertial
 322 sensors) and actuators to perform the challenging task of aerial indoor exploration. Additionally it is
 323 equipped with an onboard computer to transfer sensor and actuator data to the human robot interface via
 324 the remote connection.
- 325 •Human Robot Interface: Our human robot interface includes all software components for processing the
 326 sensory data and flight-control of the telerobot. Further it holds the interactive scene topology (RPG)
 327 which is enabled by the underlying system components (Section 4.3).

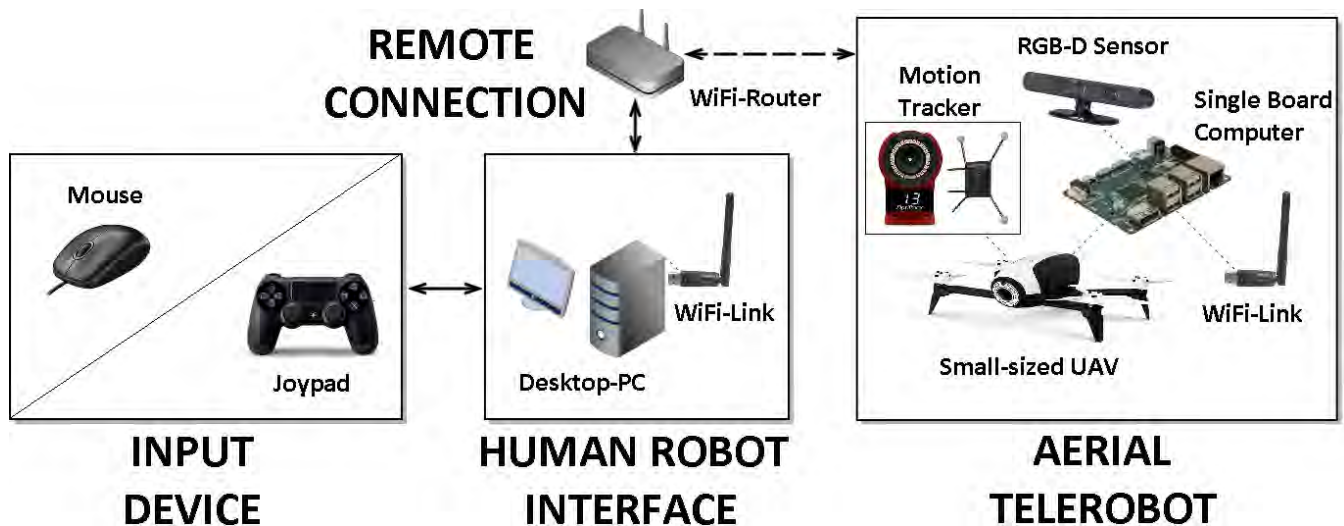


Figure 4. Overview of the main components of the teleoperation system design: The aerial telerobot which is a small-sized UAV and localized by a motion tracker (Optitrack, 2019). A remote connection between the telerobot and the human-robot interface which runs on a desktop PC. The input devices used for manual control of our teleoperation system.

328 •Input Device: The design of our system considers a simple and cost effective input device sending manual
 329 high-level commands to the human-robot interface.

330 3.1 Teleoperated Aerial Exploration Of Indoor Environments

331 Indoor space is typically limited and room exploration may require passing through narrow passages or
 332 so called portals, which can be hallways or windows. As a consequence, for our teleoperation system we
 333 designed a highly mobile and rather small sized UAV as telerobot. While important aspects are mentioned in
 334 Section 2.2, the design of our telerobot focuses on core functionalities which are vital for indoor exploration.
 335 On a higher task-level, our telerobot provides functions for **room exploration**, **object inspection** and
 336 **navigation of portals**. However, such high-level tasks entail a variety of low-level functionalities with
 337 increased complexity (Figure 5). Also, it is important to distinguish between **mission-critical tasks** and
 338 **non-mission-critical tasks**, whereas mission-critical tasks have to be solved by the teleoperation system
 339 under all circumstances and at all time. If the system fails with a mission-critical task this could lead to
 340 serious damage of the telerobot and potentially end the overall mission. For our system design we define
 341 the following low-level mission-critical tasks which are vital for indoor exploration:

342 •Localization: The telerobot has to be able to localize itself against the environment at all time. A failure
 343 in self-localization would typically result in that the telerobot collides with its environment.

344 •Landing/Take-off: Based on a robust localization and proper control of speed and acceleration, the
 345 telerobot provides assistive features like take-off and landing.

346 •Hold Position: Due to the turbulences that occur in the indoor environment, our design has to consider
 347 methods for stabilizing the telerobot while in-air and rejecting disturbances. Disturbances can occur due
 348 to flying close to obstacles or passing through portals.

349 •Collision-free Path Planning: Path- and motion-planning ensures collision-free navigation inside the
 350 indoor environment. It is vital if navigation between objects is required (waypoint-based navigation).

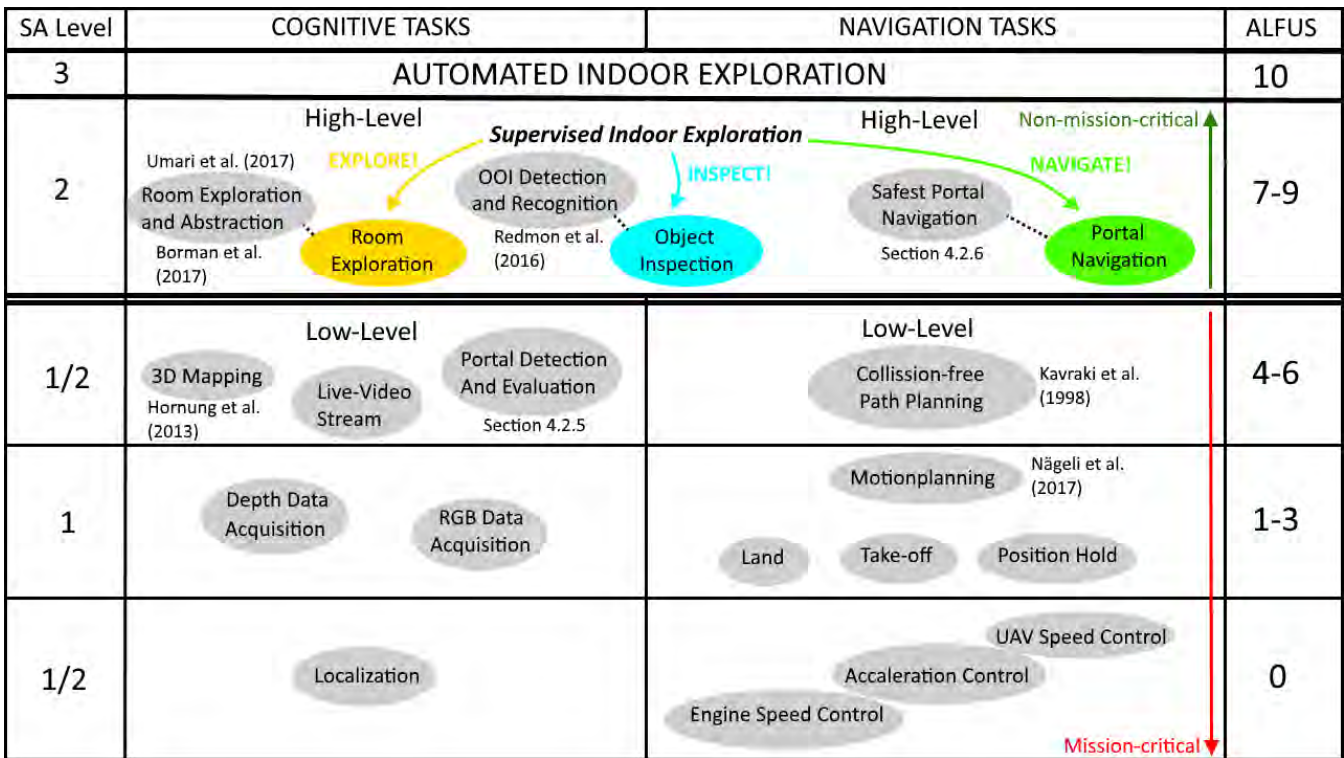


Figure 5. Overview of high-level and according low-level sub-tasks that have to be solved by our teleoperation system. Noteworthy is the separation between cognitive- and navigation-tasks, definition of mission-critical tasks, levels of situation awareness (Burke and Murphy, 2004), relation to the ALFUS (Huang et al., 2005b) and the recovery behaviours, triggered by high-level interactions of the operator (Explore!, Inspect! and Navigate!).

- 351 •Live-Video Stream And 3D-Mapping: It is based on a robust acquisition of sensory data, whereas
- 352 abstraction into a topology requires the 3D data. Since it also provides minimum understanding of the
- 353 remote scene to the human operator, these tasks must not fail.
- 354 •Portal Detection And Evaluation: We detect portals by analyzing single depth images, whereas we
- 355 recognize the contour of the portal in 3D and estimate size (minimum diameter) and the normal vector of
- 356 the contour at the geometric center. Once a potential portal is detected, it must be evaluated correctly.

357 On top of the low-level tasks we introduce high-level non-mission-critical tasks. These are difficult

358 cognitive tasks, where a human operator can still improve overall performance. The high-level tasks can be

359 summarized to one "automated indoor exploration" task, autonomously executed by the system at highest

360 LOA. In particular, the system uses an automated search strategy to explore one single room, identifies

361 objects and portals on the fly and is able to navigate the safest portal. Implementation details are given in

362 Section 4. Non-mission-critical tasks are considered as the following:

- 363 •Room Exploration and Abstraction: Room exploration is based on a state-of-the-art RRT exploration
- 364 algorithm. On lower level this requires collision-free navigation. In parallel the system has to tackle the
- 365 challenging tasks of detecting portals for navigation and objects of importance (OOIs). Once a full room
- 366 is explored it is abstracted into a node and added to the scenes topology.
- 367 •Object Detection And Recognition: For object detection our system design aims for using state-of-the-art
- 368 real-time detection algorithm.
- 369 •Safest Portal Navigation: After room exploration the system navigates the safest detected portal.

370 However, if the system fails with one of the high-level tasks, the operator can intervene by commanding
371 high-level recovery behaviours in the GUI of the human-robot interface (Figure 1). In detail the operator
372 can: trigger a simplistic but robust search strategy (**Explore!**), select a preferred portal over the other
373 (**Navigate!**) or correct for object detection by close inspecting the object and/or registering the object
374 manually (**Inspect!**) (Figure 7). Noteworthy is that our Inspect! command is motivated by the overview
375 and detail paradigm, also used in the work of Seo et al. (2017) to improve effectiveness of teleoperation.

376 3.2 Human-Robot Interface

377 Our human-robot interface is designed to support the human operator during teleoperation. Core design
378 aspects are typical essential tasks during aerial indoor exploration, limitations of the telerobot and usage of
379 an untethered remote connection.

380 3.2.1 Levels of Automation And Approaches For Control

381 Our proposed scenario for aerial indoor exploration involves rather complex tasks, like object recognition
382 and path planning. Such tasks have to be executed at the same time and involve mission-critical tasks like
383 collision-free navigation. Due to the complexity of the tasks, the design of our system assumes that true
384 full autonomy is not feasible. For our scenario a human operator is necessary to support the system with
385 complex cognitive tasks on higher level. However, these tasks are non-mission-critical. The purpose is to
386 avoid the lumberjack-effect and avoid sudden passing of control to the operator. If tasks fail on higher
387 level, the telerobot is not damaged and able to continue with the overall mission. As a consequence, in
388 accordance to related work Valero-Gomez et al. (2011), we design a supervisory control approach for
389 our system which adapts the ALFUS framework (Huang et al., 2005b). Details about task definitions,
390 high-level interactions to supervise the system with recovery behaviours and relation to LOA are presented
391 in Figure 5 and Table 2. Importantly, hazardous regions in challenging indoor environments require the
392 usage of an untethered remote connection. Consequently, potential sudden network dropouts and time
393 delays during control support supervisory control.

394 3.2.2 Graphical User Interface

395 The user interface is one vital design aspect of our full high-level teleoperation system. Moreover, its
396 design is based on the complex interplay with the underlying system components, whereas the overall goal
397 is to improve teleoperation during aerial exploration missions. Yanco et al. (2004) summarizes core design
398 aspects to improve overall task performance which are 1) using a map; 2) fusing sensor information; 3)
399 minimizing the use of multiple windows; and 4) providing more spatial information to the operator. In
400 addition, (Nielsen et al., 2007) discusses several window layouts in a standard paradigm. Besides of the
401 rich variety of designs found in related work, a very common window layout is placement of exocentric
402 map views on the bottom half of the screen whereas egocentric live camera views are placed on top.

403 The design of the GUI is also based on a standard layout, whereas we keep all view windows at equal
404 size. It includes a traditional egocentric live view on top and a 3D map view on the bottom half of the
405 screen. The purpose is to provide a minimum of spatial understanding to the operator. For the 3D view
406 we use grid-map representations as they are a more robust in the presence of network delays and sudden
407 dropouts (Riestock et al., 2017b). We place the view of the interactive scene topology (RPG) side by side to
408 the traditional views to avoid occlusions or switching. The RPG is motivated by exploration of structured
409 human environments, which can have complex and repetitive geometry (e.g. office buildings). While the
410 structure of such environments motivates a topological representation of the environment, related work
411 (Section 2.4.2) clearly supports the use for navigating robots. Other motivational aspects are extensively

412 discussed by Johnson (2018). Amongst other benefits, the work states that a topological representation
413 is suitable for telerobots which have to navigate reliably from one place to another without the need of
414 building an accurate map. While this is not valid during exploration of the environment, clear benefits occur
415 for repeated navigation from one object to another after exploration. Johnson (2018) also points out that
416 the topology supports affordances (opportunities for interactions) and poses a human-like representation
417 of the environment. Based on the concept of an ecological interface (Nielsen et al., 2007), we designed
418 visualization of objects that support affordances, but do not overwhelm the operator (Atherton and Goodrich,
419 2009). Consequently, we define general OOIs, which are detected during the exploration mission and
420 highlighted in the topological scene view. Based on these considerations and avoiding to overwhelm the
421 operator with too rich scene details in the traditional views (left and middle Figure 3), our design leads to
422 the RPG which poses an interactive topological 2D map of the indoor environment. Implementation details
423 can be found in Section 4.2.

424 3.3 Input Device

425 The design of our high-level teleoperation system includes a topological scene view which is represented
426 in 2D. Because the topology supports affordances, we make OOIs explicit for interaction during flight.
427 Motivated by the 2D representation and also considering the design aspects discussed in Section 2.5 we
428 consequently selected a 2D mouse as input device. Besides of being robust and simple to setup (e.g., no
429 need for calibration), other advantages are shorter pre-training phases and cost-effectiveness (Espingardeiro,
430 2012). The mouse holds three buttons, whereas the operator can trigger three high-level recovery behaviours
431 (Figure 1 and Figure 9) of the aerial telerobot (Section 4.1).

4 SYSTEM IMPLEMENTATION

432 To solve the challenging tasks that occur during aerial indoor exploration missions, we implemented the
433 following components as part of our high-level teleoperation system:

- 434 • **Aerial telerobot** represented as small-sized UAV. The UAV is equipped with a sensory setup to acquire
435 RGB-video and depth data. The data is transferred to a desktop PC via the remote connection.
- 436 • **Human-robot interface** to facilitate control of the aerial telerobot by providing different views of the
437 remote scene. Based on these views the operator controls the telerobot in a supervisory manner via
438 high-level interactions. It further holds the underlying system components that are responsible for flight
439 control, 3D mapping, abstraction, detection of portals and object detection in real-time. Remarkably, the
440 components are vital for enabling the interactive scene topology of the human-robot interface. Thus, they
441 are also essential to enable the high-level interactions (Explore!, Inspect!, Navigate!).
- 442 • **Input devices** that sends manual inputs to the human-robot interface. It is implemented as a simple and
443 cost-effective mouse to interact with the RPG. To compare our system against traditional controls, we use
444 a joystick controller for our user study (Section 6.1).

445 While the physical setup of the teleoperation system is shown in Figure 6, we give an overview of the
446 software implementation represented as state diagram in Figure 7.

447 4.1 Aerial Telerobot (UAV)

448 For the aerial telerobot (UAV) of our system we use a modified Parrot Bebop 2 (Parrot, 2015). It is compact,
449 suitable for narrow indoor spaces and offers open-source drivers (Monajjemi, 2015) for low-level flight
450 control. For reliable experimentation, we attach retro-reflective markers for outside-in localization using

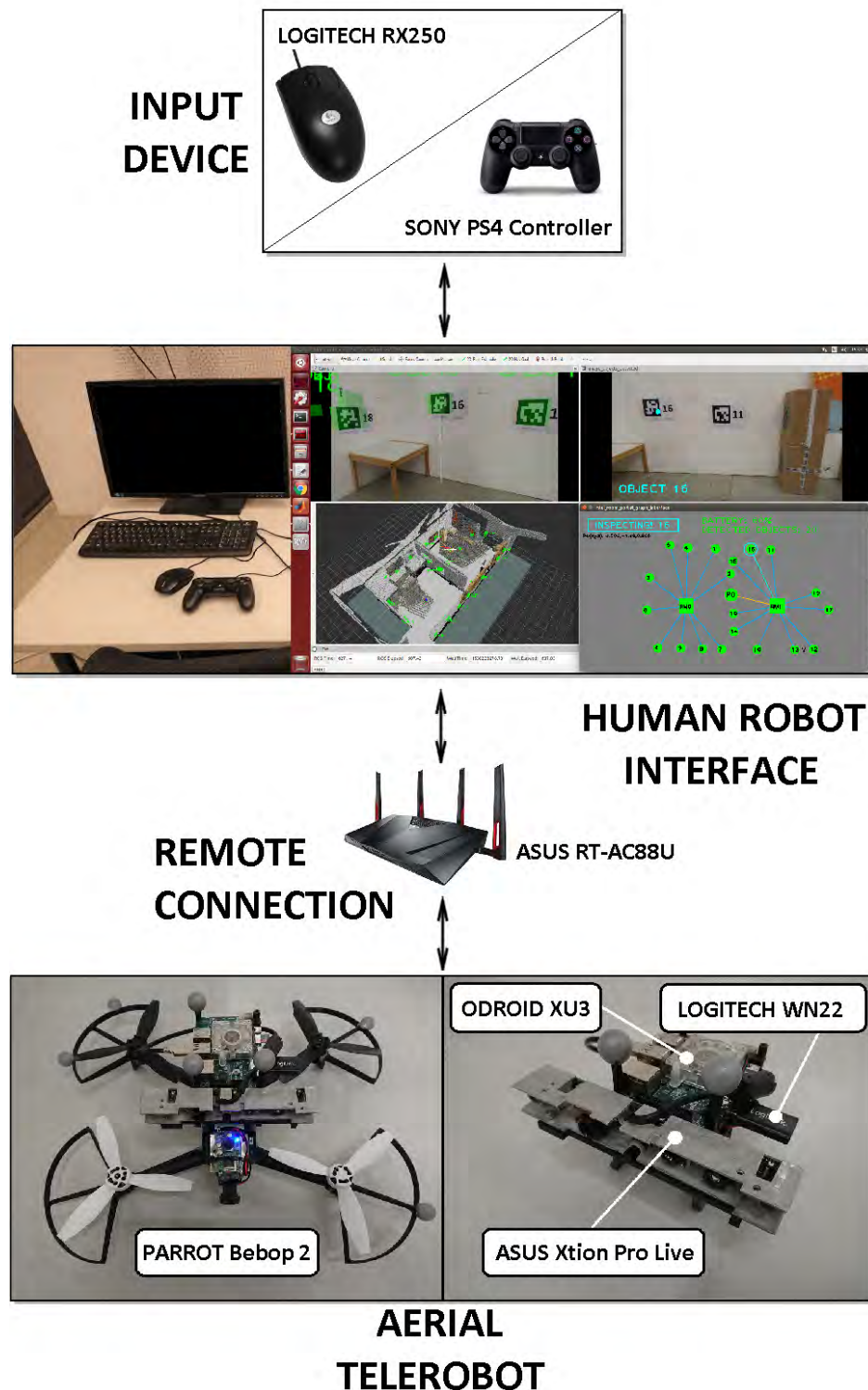


Figure 6. Implementation of the main components of the high-level teleoperation system: The UAV based on a Parrot Bebop 2 with onboard single-board-computer and sensory setup. The remote connection implemented as ASUS RT-AC88U wireless router. The GUI, including the RPG, implemented on a desktop PC in ROS. The input devices implemented as a Logitech RX250 mouse and a PS4 controller.

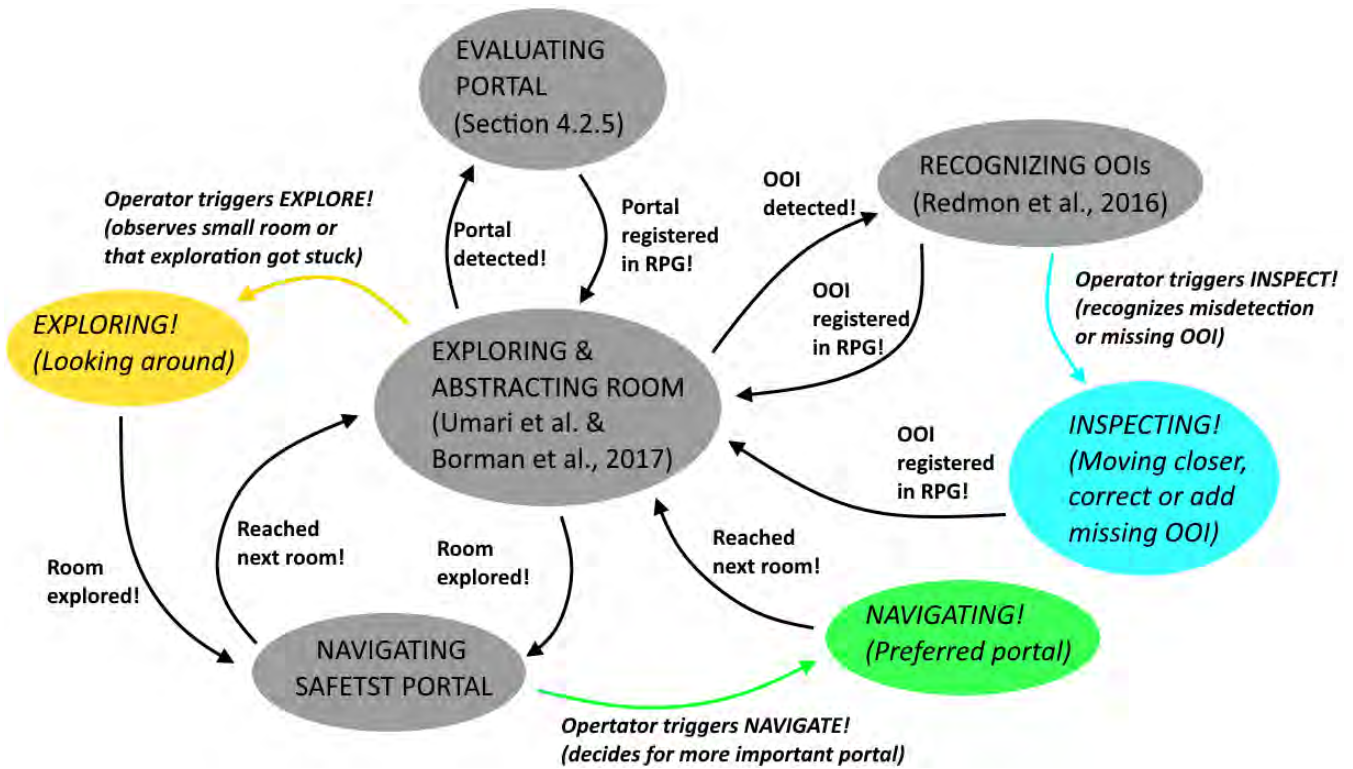


Figure 7. State diagram of the software framework of our teleoperation system.

451 an Optitrack Flex 13 infrared motion capturing system. An overview of the physical setup is shown in
 452 Figure 6.

453 With all on-board sensors attached, the outer dimensions of the UAV are $32.8 \times 38.2 \times 25\text{cm}$, and it
 454 weighs 700g , with flight times of up to approx. 10 minutes. On top of our UAV, we mount a customized
 455 RGBD sensor rig (250g), consisting of an ASUS Xtion Pro Live sensor ($FOV_{hor.} = 58^\circ$, $FOV_{vert} = 45^\circ$)
 456 and a Logitech WN22 WiFi stick, connected via USB to an ODROID XU3 single-board computer. During
 457 our experiments, the UAV was navigating at a default flight height of $z_{takeoff} = 1.25\text{m}$.

458 **4.2 Human-Robot Interface And Input Devices**

459 In this section, we give details about the human-robot interface which enables the operator to high-level
 460 control our teleoperation system. As one vital component it holds the RPG as interactive scene topology
 461 which is created, based and, thus, strongly dependent on the complex interplay of its underlying system
 462 components (Section 4.3). While we motivate a supervisory control approach in Section 3.2.1, in the
 463 following we discuss implementation details and the correspondence to the LOA. Furthermore, we give
 464 details about the traditional baseline system with a joystick as input device in Section 4.2.2. It runs on
 465 low automation level, and the operator has manual control over the system. We compare the two different
 466 systems against each other and report on results in Section 6.1.

467 **4.2.1 High-Level Teleoperation (RPG Condition)**

468 High-level teleoperation of our system is enabled by the RPG to let an operator effectively supervise our
 469 system on high LOA (Table 2). We intentionally do not provide low-level access, so that the operator is
 470 not burdened with demanding mission-critical tasks (ALFUS 1-6). This also means that the system must
 471 achieve all mission-critical tasks even in a challenging indoor environment. The system usually operates on

472 highest LOA (ALFUS 10), but we let the operator switch to a lower collaborative level (ALFUS 7-9), if
473 supervision is required. This is particularly relevant if the underlying system components components do
474 not perform satisfactorily, e.g., when object recognition fails (Materna et al., 2017).

475 For the RPG (Figure 2), we combine a traditional egocentric view (on-board camera of the UAV) with an
476 exocentric 3D map view. The views include visual aids for current pose of the UAV, view frustum of the
477 onboard camera, the online reconstructed 3D environment and invalid flight zones. The purpose is provide
478 a basic spatial understanding of the scene. We extend the ego- and exocentric views with an interactive
479 topological view, the RPG. It consists of rooms (nodes) and portals (edges) to other rooms or OOIs (e.g., a
480 fire extinguisher or a victim). OOIs registered in the RPG are highlighted in real-time. Once an interactive
481 OOI is highlighted, the operator can use 2D mouse inputs to supervise the system by a reduced set of
482 high-level interactions (**Explore!**, **Navigate!** and **Inspect!**). This triggers recovery behaviours (Figure 9
483 and implies switching from highest LOA (ALFUS 10) to collaborative level (ALFUS 7-9).

484 The Explore! command lets the system more effectively uncover smaller rooms. During this task, our
485 system autonomously detects OOIs and adds them as interactive nodes to the RPG topology. If a false
486 detection occurs, the operator can use the Inspect! command to move closer. If one of the detected objects
487 is selected, a safe path is generated between the current location of the UAV and the object. After the
488 system navigates close to the false detection, the operator can inspect the situation in a close-up egocentric
489 view and determine further action. During exploration of a room, also portals which are safe for navigation
490 are detected and highlighted (Section 4.3.4) automatically. Detected portals add a new node and edge to the
491 RPG. In case of multiple detections, the operator is able to select a preferred portal to trigger navigation
492 into the adjacent room (Navigate!). A picture sequence of the recovery behaviours is shown in Figure 9,
493 whereas we present real-world flights in our supplementary video (Section 7). Details about the physical
494 setup of the aerial telerobot are discussed in Section 4.1.

495 The goal of the RPG is to provide a topological map that is a human-like representation of the environment.
496 Since it provides natural interactions for commanding the system and describing the environment, it
497 facilitates and eases human-robot-interaction Johnson (2018). Moreover, its purpose is to reduce scene
498 details in the presence of cluttered traditional views (left and middle Figure 3). However, the concept of the
499 RPG has also limitations which we detail in Section 5.

500 4.2.2 Traditional Direct Teleoperation (JOY Condition)

501 To compare the effect of our high-level teleoperation system against a state-of-the-art baseline system, we
502 implemented traditional joystick controls. For our study we define it as condition JOY. In this condition,
503 the operator uses a joypad to command the UAV at lower ALFUS (Table 2) with a high-level of interaction
504 on sides of the human operator (ALFUS 1-3). At this level, the system takes care of automatic take-off,
505 position stabilization and landing. Besides, the operator is also responsible for mission-critical tasks.

506 To achieve fair comparison against the RPG, we added a visualization of flight zone boundaries to help the
507 operator prevent collisions. The boundaries are displayed in the horizontal plane via a color-coded surface
508 at the height of the UAV. Operators must not exceed this indicated boundary and get color-coded feedback,
509 if they are close to exceed the maximum flight height. The surface turns orange, if the UAV is close to the
510 height boundary, which means the distance of the geometric center of the UAV to the upper boundary is
511 smaller than the height of the UAV. The surface turns red, if the distance is smaller than half of the height
512 of the UAV, indicating that the operator has to steer the UAV downwards immediately.

513 The joystick is used in MODE-2 configuration, allowing the operator to give direct motion commands. In
514 this configuration, the left rudder stick controls translational and rotational velocity of the z-axis of the
515 UAV, and the right rudder stick gives acceleration inputs along the x-axis and y-axis of the UAV.

516 4.3 Underlying System Components

517 This section summarizes the underlying components of our high-level teleoperation system. They are
518 implemented as part of the human-robot interface on a Desktop PC and responsible for exploration, flight
519 planning and navigation, 3D mapping of the environment and highlighting of OOIs. Since they even
520 enable the RPG as interactive scene topology, the effectiveness of our full system strongly depends on their
521 performance. Thus, they must be emphasized as core for interaction. The aerial telerobot supports with
522 automated indoor exploration and the human operator can trigger recovery behaviours via the RPG. In
523 order, if a non-mission-critical task fails, time performance could be improved. The recovery behaviours
524 are designed in a supervisory manner so that the human operator can effectively supervise the system with
525 difficult tasks on higher-level. Their purpose is emphasized throughout the following use cases:

- 526 •Explore: After take-off, the UAV autonomously starts exploring the current room using an RRT-based
527 exploration method (Umari and Mukhopadhyay, 2017). If the operator decides that the room seems
528 rather small or the exploration fails to fully explore the room, the operator can on demand trigger a
529 simple recovery behaviour. In that case the UAV explores the local environment by flying a simple
530 circular trajectory. Once a room is fully explored we use the implementation of Bormann et al. (2016) for
531 room-segmentation.
- 532 •Inspect: During exploration of a room, the telerobot autonomously detects portals and OOIs, like victims
533 or fire-extinguisher. However, if the operator feels that an object was misdetected, the operator can
534 command the telerobot to move closer to a detected OOI or portal for verification.
- 535 •Navigate: During room exploration, the telerobot detects portals which are safe to navigate. However, if
536 multiple safe portals are detected, the human operator might intuitively prefer one portal over the other
537 for navigation. In such cases the operator can manually trigger portal navigation.

538 4.3.1 Room Exploration

539 At the beginning of every mission, the UAV ascends to a default flight height (Section 6.1). After reaching
540 the default height, the system starts to autonomously explore the local environment (Figure 8, Step 1).
541 For local exploration of a single room, we use a frontier detection algorithm, based on rapidly-exploring
542 random trees (Umari and Mukhopadhyay, 2017). If no failure cases occur, we consider the system to work
543 on highest LOA (ALFUS 10).

544 Once the UAV takes off, we start detection of local frontiers by taking into account the occupancy map
545 constructed online. First, we project 3D occupancy information into 2D, since this helps to clearly define
546 boundaries of a single room. We project occupied cells into the 2D map. Second, we let a local frontier
547 detector discover valid navigation points, which are derived from a rapidly growing random tree biased
548 towards unexplored regions of the occupancy map. Third, we directly steer the UAV towards the detected
549 point, incrementally exploring the local environment. These steps are repeated, until no new frontier points
550 are detected and the room is locally fully explored. To abstract the local room and to further obtain room
551 information we make use of the segmentation approach presented by Bormann et al. (2016). Note that
552 we assume the range and FOV of our depth sensor to be wide enough to cover the close environment and
553 detect potential obstacles, when navigating at default height. For simplicity, we assume that there are no
554 additional obstacles between the UAV and the detected room boundaries. The operator is further able to

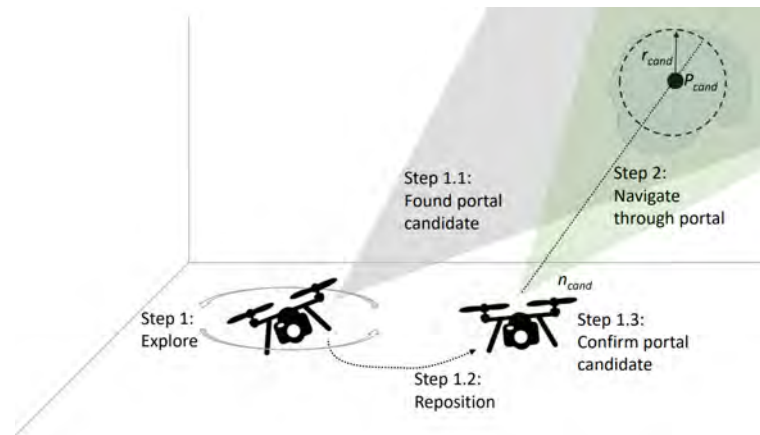


Figure 8. Method for detecting and evaluating potential safe portals directly from depth-image data. The UAV first explores the close environment and, if a safe-portal candidate is detected, positions itself to confirm that the portal candidate is safely traversable.

555 manually override frontier detection by selecting the abstract room representation of the RPG (triggering
 556 Explore! and switching from highest- to collaborative LOA). This prompts the system to execute a more
 557 efficient circular trajectory.

558 4.3.2 Room Navigation

559 To enable collision-free navigation through portals from one room to another, we use a global path planning
 560 approach based on probabilistic road maps (PRM) (Kavraki and Latombe, 1998). The global path planner
 561 generates a PRM based on the occupancy grid map (Hornung et al., 2013). The PRM is represented as a set
 562 of 3D points given in world coordinates. For an example of generated paths, please refer to Figure 9c.

563 The PRM is passed to a real-time motion planning framework Gebhardt et al. (2016); Nægeli et al.
 564 (2017b,a). The motion planner involves a model predictive controller (MPC), which produces smooth
 565 motion trajectories for the UAV when moving along the global path. Following a receding-horizon MPC
 566 formulation, at each timestep Δt , a locally optimal path with N steps and a duration of $N\Delta t$ is computed.
 567 This optimization problem is re-evaluated at every sampling instance T_s , leading to a closed-loop behavior.
 568 Thus, we make use of the disturbance rejection characteristics of the MPC to stabilize the UAV during
 569 the mission. Stabilization against turbulence is necessary when flying close to objects or passing through
 570 portals. The real-time motion planner is implemented in MATLAB (Robotics Toolbox), utilizing the
 571 FORCES Pro real-time solver (Domahidi and Jerez, 2013).

572 4.3.3 Environmental Reconstruction

573 To provide the operator with basic environmental understanding during navigation (Section 4.3.1), we
 574 make use of the RTABMap reconstruction framework (Labbe and Michaud, 2013, 2014). It represents the
 575 reconstructed geometry as a colored occupancy grid map and is capable of loop-closure detection. The grid
 576 map is created by fusing depth- and RGB-data from the onboard sensor setup of the UAV (Figure 6) and
 577 visualized in the exocentric view.

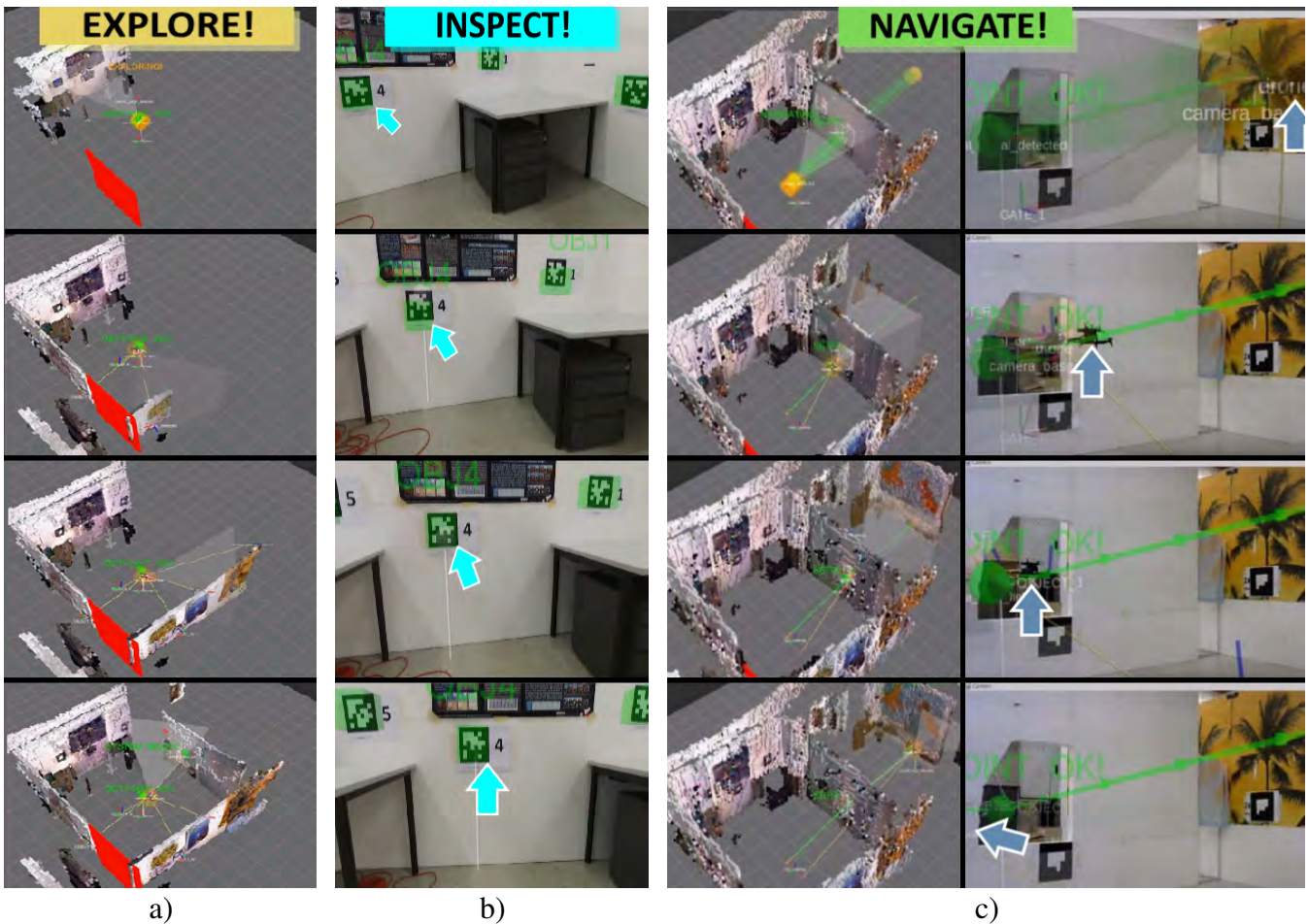


Figure 9. Exocentric virtual views of the aerial robotic system during execution of the recovery behaviours. a) The UAV is commanded to explore its surrounding by flying a circular trajectory and simultaneously builds a 3D model of its environment from RGBD data. b) The UAV is commanded to close inspect a detected object for verification. c) The UAV is commanded to navigate through a safe portal to the adjacent room along an autonomously planned path, shown in green. The UAV's position is marked with blue arrows.

578 4.3.4 Detecting And Highlighting Objects Of Interest

579 For our experimental setup, we introduce different types of OOIs which are commonly present in exploration
 580 scenarios. These objects can be hazardous areas (location of fire extinguishers, broken power lines, gas
 581 leaks), human victims (embodied by human-like mannequins) or portals (potentially narrow passages),
 582 which connect adjacent rooms. The OOIs are automatically highlighted as virtual overlays in the GUI
 583 to direct the operators attention towards them. This requires automatic object detection and registration
 584 of the observed object positions in world coordinates. Noteworthy, we use a true relative scale between
 585 objects in the current design of the RPG. We detect objects either using the YOLO framework for object
 586 detection (Redmon et al., 2016) or by simply marking them with Apriltag markers (Olson, 2011) during
 587 the user study (Section 6.1).

588 Indoor environments can typically be structured into wider open areas (rooms) and more narrow spaces
 589 (portals) connecting rooms (Kun et al., 2017). During the exploration task, our goal is to detect and
 590 visualize potential portals. Making rooms and portals explicit is vital in our scenario, since they support
 591 navigation. Interactive highlighting, helps operators to get a clearer understanding of the environment and
 592 make an educated decision on which part of the environment to explore next. The portal detection proceeds

593 as follows (Figure 8): During exploration of the close environment (Step 1), we detect discontinuities
 594 in the depth images captured by the RGBD sensor. If the discontinuities form a closed, bounded region
 595 with minimum radius r_{cand} and depth d_{min} (measured from the centroid P_{cand} of the entry surface),
 596 the region is selected as a portal candidate (Step 1.1). This intermediate step is necessary to ensure the
 597 portal can be safely traversed, as looking at portals from larger offset angles would result in shadowed
 598 regions behind the portals. Based on the surface geometry of the portal candidate, we derive P_{cand} and
 599 the corresponding normal vector \vec{n}_{cand} . The normal \vec{n}_{cand} is oriented perpendicularly to this entry surface
 600 and has its origin in P_{cand} . In Step 1.2, the UAV is commanded to align the x-axis of its local coordinate
 601 frame F_{UAV} with \vec{n}_{cand} . The distance to the portal candidate d_{cand} is calculated based on the minimum
 602 radius r_{cand} and the narrower vertical field of view of the depth sensor FOV_{vert} . d_{cand} can be expressed as
 603 $d_{cand} = r_{cand} / \tan(FOV_{vert})$.

5 SYSTEM LIMITATIONS

604 The teleoperation system presented in this work has also several limitations. Besides of typical issues
 605 related to telerobotics as such, most important limitations are discussed in the following:

- 606 •Telerobot: Besides of there is room for improvement of our physical design (weight, size and
 607 computational onboard power), also the ability to morph and adapt to challenging environments could be
 608 added. Speaking of passing narrow portals or gaps, also highly dynamic maneuvers (Falanga et al., 2017)
 609 are currently not possible but could be interesting for future work. Another limitation of the telerobot is
 610 the exploration algorithm. While we make use of an RRT-based approach to explore a single room but
 611 at constant flight height, a more powerful approach would involve full 3D exploration. Additionally, a
 612 gimbal could help to resolve constraints with the cameras limited FOV, making room exploration more
 613 efficient.
- 614 •Wireless Remote Connection: Due to the usage of an untethered remote connection between the
 615 telerobot and the human-robot interface, typical problems could occur like limited bandwidth and sudden
 616 connection dropouts. While in-field applications would require a much more sophisticated (and expensive)
 617 setup, in our implementation we considered commodity hardware only. However, it must be stated that
 618 due to usage of a powerful WiFi router, comparably short ranges, and non-overlapping/non-populated
 619 channels the effects during the user study could be reduced to a minimum.
- 620 •Supervisory Control of high-level tasks: The supervisory control approach of our system aims for
 621 effectively resolving failures of high-level tasks. However, this is only valid if the telerobot is capable of
 622 handling all low-level mission-critical tasks without failure.
- 623 •Human-Robot Interface: An essential component of our human-robot interface is the RPG, serving as
 624 interactive scene topology. The focus of its design is to supplement traditional views by supporting
 625 affordances and reducing scene detail. Thus, overwhelming the operator should be avoided. However,
 626 several aspects could not be elaborated on as part of this work. While in our current RPG design we use a
 627 true relative scale of rooms, portals and objects, we did not elaborate on different layouts of the objects
 628 inside the RPG view or adapting its orientation relative to the 3D view. We also did not yet investigate on
 629 proper placement of the simplistic 2D objects in case they overlap or on altering their shapes and size.
 630 Future work would also include elaboration on a zooming function for wider areas and adding important
 631 details on demand. Such helper functions could display size and volume of the selected room or distance
 632 between the telerobot and according OOI if selected with the input device.
- 633 •Input device: The design of our teleoperation system supports a robust and simple-to-use input device
 634 which is also cost effective. As a consequence we utilize a traditional 2D mouse with 3-buttons. These

635 are dedicated to our three high-level interactions (Figure 1 to trigger recovery behaviours. However,
636 the design of interactions and button mappings could be still improved by evaluating different layouts
637 towards optimum usability. Further, utilizing a mouse with more degrees of freedom (Razor, 2015) could
638 improve support for multi-floor exploration or manual steering of a camera gimbal with the attached
639 joystick.

640 •Multi-floor environments: To be able to explore multi-floor environments, our system would require
641 further components. For instance, the system would need to be able to detect stairways (Delmerico
642 et al., 2013). In addition, the robustness of the untethered remote connection would have to be improved.
643 While the implementation of our current system uses commodity hardware, systems with increased
644 power and higher penetration of structures are for example presented by Patra et al. (2007). Additionally,
645 like introduced for nuclear power plant inspection (Nagatani et al., 2013; Zhang et al., 2018), one or
646 multiple additional telerobots could be used as mobile wireless transmission relays, retaining reliable
647 communication.

6 USER STUDY

648 The purpose of our study is to investigate the effect of our high-level teleoperation system on operator
649 performance during real-world exploration missions. We considered the different teleoperation systems
650 as strongest baseline for our study conditions, whereas we compare our high-level teleoperation system,
651 including the RPG (Section 4.2.1), against a traditional baseline system with direct controls (Section 4.2.2).
652 Table 1 gives an overview of the experimental conditions, type of systems, and view modes.

653 A core aspect of our study is that, despite a variety of related work has shown semi-autonomous systems
654 positively effecting task performance, however it is unclear if this holds in a realistic setting where a system
655 has to generate an interactive abstract topological scene view in real-time during flight missions. While
656 operators with traditional direct controls can issue commands based on their quasi-instantaneous human
657 cognition, operators of the semi-autonomous system need to wait until it processes, abstracts and outputs
658 (visualizes) the abstracted information. This raises the question if such systems are still able to improve
659 task performance over traditional control approaches in a realistic setting, where operators potentially need
660 to wait until information is available in the topological view.

661 6.1 Experimental Design

662 In the following sections we summarize the experimental design of our user study, including study
663 conditions and tasks. Besides, we give details about study procedure, participants and accordance of the
664 study to the local legislation.

665 6.1.1 Conditions

666 The main objective of our study was to assess the effect of the two user interface conditions, RPG and
667 JOY, on operators task times, mental load and general comfort during a real-world indoor exploration
668 mission. We based our study on **within-subjects design** and varied the order of the conditions using **full**
669 **counterbalancing**. We defined task completion time, mental load and general comfort of the operator as
670 main task performance metrics. We formulated the following hypothesis for the user study and report on
671 results in Section 6.2:

- 672 •H1: The operator's task time decreases in RPG.
- 673 •H2: The operator's mental load decreases in RPG.

674 •H3: The operator's general comfort increases in RPG.

675 6.1.2 Tasks

676 According to Bhandari et al. (2015), typical indoor exploration tasks involve investigation of the unknown
677 environment and evaluation of hazardous areas to minimize human risk. We designed our study so that
678 participants had to fulfill similar tasks in our experimental setup (Figure 11). We assumed a situation where
679 the operator is far from the indoor space and has no prior knowledge of it. To ensure a basic degree of
680 validity, we discussed the design of our experimental task-design with a local fire brigade. As a conclusion,
681 the members confirmed validity of our task design and further emphasized usefulness of our system for
682 assessment of a stable but still potentially dangerous situation. As an example use case, they specified the
683 on-site inspection of a damaged chemical recovery boiler where an imminent explosion cannot be ruled
684 out.

685 The indoor exploration task of our study comprises three subtasks, which had to be completed by each
686 participant in each of the conditions. During this task, participants had to fully explore the environment
687 and find all OOIs. In particular, participants were told to:

- 688 •Find all 19 hazardous areas marked with fiducial markers.
- 689 •Find the safe portal.
- 690 •Find the victim.

691 The placement of objects was altered in a controlled fashion to avoid learning effects. An overview of the
692 experimental indoor environment is given in Figure 11.

693 6.1.3 Procedure

694 Before each experimental session, an introduction to the teleoperation system was given to the participant
695 by the experimenter. Preliminary questions were asked to identify eye-sight restrictions. The evaluation
696 procedure of each experimental condition can be split into three phases. In a training phase, participants
697 learned to use the system of the specific condition. This phase ended when participants reported to be
698 comfortable in using the system. In the second phase, participants had to accomplish the indoor exploration
699 task as fast as possible. For each participant, we captured screen recordings and measured the task
700 completion time using a stop watch. The task was considered to be completed when the system detected all
701 safe portals, hazardous areas and victims (RPG-condition) or users verbally confirmed to the experimenter
702 that they found all of those objects (JOY-condition). In both conditions, users were aware of the number
703 of objects they already identified as well as of the objects they still need to find. Finally, participants
704 were asked to fill out a NASA-TLX (Hart and Staveland, 1988) task-load questionnaire (Scale: 0-100) as
705 well as a custom questionnaire with respect to their experience in the respective condition. The custom
706 questionnaire contained 8-point Likert items (ranging from 1, "strongly disagree", to 8, "strongly agree")
707 asking participants about accuracy and smoothness of control as well as their perception of control over the
708 system and their general comfort during the task.

709 6.1.4 Participants

710 A total of 23 participants were invited, 20 of them successfully finished the given tasks in all conditions.
711 3 participants had to stop the study due to technical problems and their results have been excluded. We
712 invited 17 male participants and 3 female participants which were either students or researchers in the field
713 of computer science or electrical engineering at Graz University of Technology (age: $M=27.6$, $SD=3.98$).

714 6.1.5 Ethics Statement

715 The presented study was carried out in accordance with the World Medical Association's Declaration of
 716 Helsinki, as revised in 2013 (HELSINKI, 2013). The study did not involve any medical experiments and
 717 further, no biometric data was taken from participants. We did not take any personal data from participants
 718 besides of participants age, whereas all taken data was fully anonymized. In general, the study was
 719 conducted in accordance with the local General Data Protection Regulation (GDPR) in Austria and all
 720 participants gave written informed consent via an IRB consent-form. In order, as per the local legislation,
 721 no IRB approval was required for our particular study type.

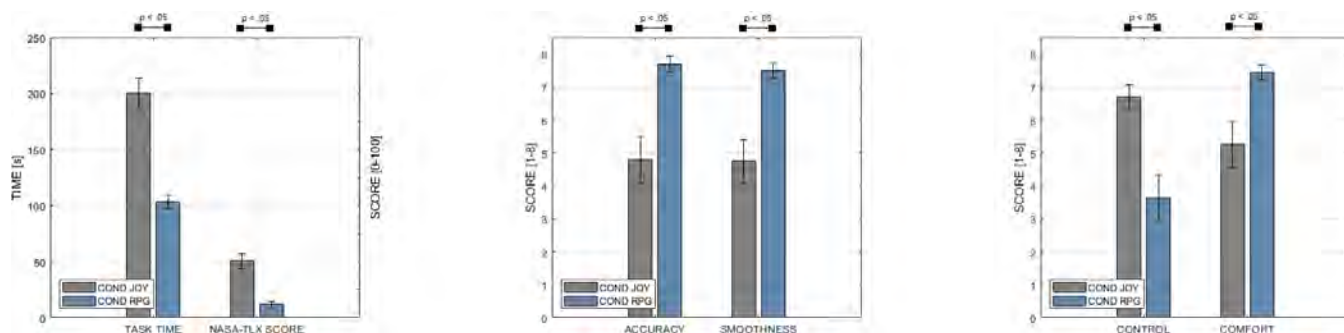


Figure 10. Our study results indicate significantly decreasing task times (Scale: 0-250s) and decreasing NASA-TLX score (Scale: 0-100) with our high-level teleoperation system (condition RPG). Based on an even 8-point Likert scale (Agreement-Scale: 1 Strongly Disagree - 8 Strongly Agree), we managed to retain general comfort during operation, compared to our baseline system with traditional joystick controls (condition JOY). In addition, participants reported increasing accuracy of control and smoothness of control.

722 6.2 Results

723 In each of our 20 sessions, we tested the teleoperation system in both conditions, JOY and RPG. This
 724 resulted in a total of 40 valid runs. For each participant, we took screen recordings and measured the task
 725 completion time during the flight. After finishing the flight for one condition, participants were asked to fill
 726 out the NASA-TLX score as well as a custom questionnaire. This questionnaire contained several 8-point
 727 Likert items asking participants about the accuracy of control, the smoothness of control, their perception
 728 of control over the system and their comfort in general during the task. We report mean, standard deviation
 729 and interval estimates for a 95% confidence interval. For significance testing, we use a paired samples
 730 t-test for task execution time as the data is normally distributed. All other measures are compared using
 731 Wilcoxon signed-rank test as questionnaire responses are non-parametric.

732 The main findings of our study are summarized in Figure 10. Statistical testing revealed that the task
 733 completion time was significantly lower for the RPG- ($M = 103.7s, SD = 13.7s$) compared to the
 734 JOY-condition ($M = 200.1s, SD = 30.58, t(19) = 12.01, p < 0.001$). In addition, a significant effect of
 735 conditions on mental load, as determined by NASA-TLX, has been revealed ($Z = 210.0, p < 0.001$). Again,
 736 RPG ($M = 11.75, SD = 6.43$) caused a significantly lower mental load than JOY ($M = 50.71, SD =$
 737 16.41).

738 In our custom questionnaire, we asked participants about their perception of the tested user interface.
 739 Unsurprisingly, the perceived level of control in conditions decreased with the increasing LOA from
 740 JOY ($M = 6.7, SD = 0.87$) to RPG ($M = 3.65, SD = 1.63$). Wilcoxon signed-rank test showed that

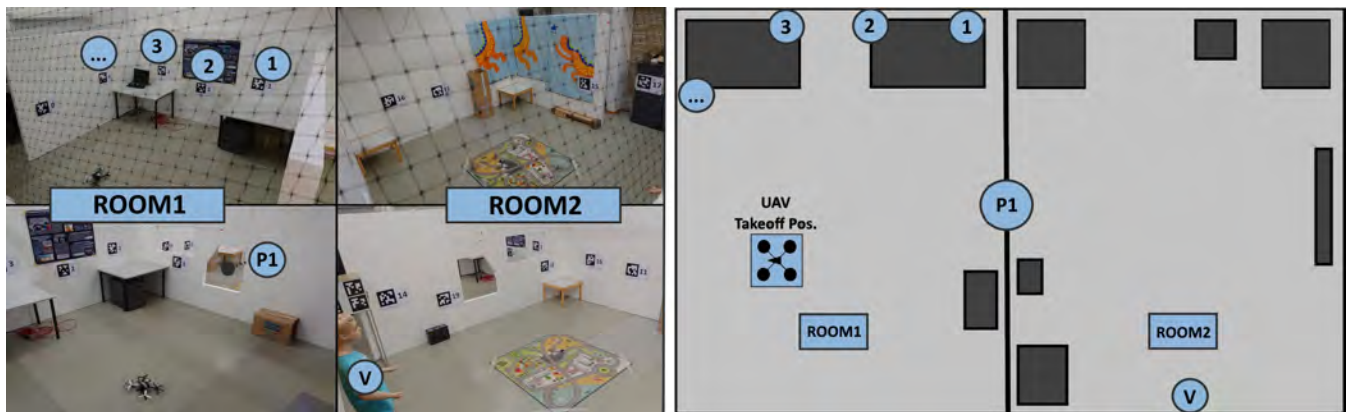


Figure 11. (left) Physical setup for our experimental evaluation. Note the two rooms, connected via a safe portal and the objects of interest including a victim. (right) The same environment, represented as a floor-plan in 2D.

741 these differences are significant ($Z = 169.0, p < 0.001$). In contrast, participants perceived RPG ($M =$
 742 $7.7, SD = 0.57$) to be significantly more accurate than JOY ($M = 4.8, SD = 1.67, Z = 0.0, p < 0.001$).
 743 Similarly, perceived smoothness of control was higher for RPG ($M = 7.5, SD = 0.51$) compared to
 744 JOY ($M = 4.75, SD = 1.55$). Again, differences are significant ($Z = 0.0, p < 0.001$). Finally, perceived
 745 general comfort was significantly higher in the RPG condition ($M = 7.45, SD = 0.51$), compared to
 746 JOY ($M = 5.25, SD = 1.62$), with ($Z = 0.0, p < 0.001$). This lets us accept H3, which is supported
 747 by a significantly higher task completion confidence in RPG ($M = 7.8, SD = 0.41$), compared to JOY
 748 ($M = 6.8, SD = 1.06, Z = 0.0, p < 0.001$).

749 6.3 Discussion

750 Overall, we were able to support all of our three hypotheses, implying that our high-level teleoperation
 751 system is successful in supporting the operator during aerial exploration missions in challenging indoor
 752 environments. Remarkably, our teleoperation system reduced task execution times by 48.28% and task
 753 load by 76.82% compared to the JOY condition. Moreover, results indicate an increase in general comfort
 754 by 41.90%. We attribute the significant differences between conditions to the interplay of the RPG-view
 755 and the autonomous system. However, further research is necessary to differentiate the influence of the
 756 autonomous system and the topological scene view on results.

757 Although, participants conducted real-world flights to solve the posed exploration task, the study took place
 758 in a controlled environment. For instance, localization of the UAV was achieved with a motion capture
 759 system. However, on-board localization methods like SLAM have proven to be sufficiently accurate and
 760 fast to be used for UAV position estimation (Weiss et al. (2011), Mur-Artal and Tardós (2017)). In addition,
 761 due to limited lab space, the environment of our study did only comprise two rooms. Nonetheless, we
 762 believe that differences between conditions further evolve in favor of our system in wider- or multi-floor
 763 environments. The reason is that it is evidently harder to gain a good spatial understanding of larger
 764 compared to smaller environments. Thus, operators will benefit more from the RPG-view in larger spaces
 765 as it abstracts the environment in an easy-to-understand manner. Furthermore, the task of our study was
 766 a simplification of complex real-world search and rescue missions. However, it is likely that our system
 767 even better supports operators in more complex task scenarios. For instance, research has shown that
 768 topological views, like the RPG, are beneficial if an environment is fully explored and operators are required
 769 to repetitively navigate between OOIs Johnson (2018). With regards to our system, the reinspection of

770 an OOI could easily be performed by triggering its visualization in the RPG. The telerobot would then
 771 autonomously renavigate to the specific room and object. Due to mentioned reasons, we argue that, despite
 772 limitations, our experimental setting is an ecologically valid approximation of a real-world exploration
 773 mission.

774 Summarizing, our study has shown that high-level teleoperation systems with an on-the-fly created
 775 interactive scene topology are still able to better support operators in real-world settings, compared to
 776 systems using traditional controls.

7 CONCLUSION AND OUTLOOK

777 In our work, we demonstrate a fully working teleoperation system for aerial exploration missions. It
 778 improves task performance by using an interactive scene topology, whereas related work motivates using
 779 topological representations for robotic teleoperation. However, in contrast to related work, we for the
 780 first time investigate on how task performance is effected if the topology is created in real-time during
 781 actual flight missions. The overall goal of our system was to reduce task times and mental load of the
 782 operator while conserving general comfort. To elaborate on the expected improvement, we evaluated
 783 our teleoperation system with a user study under real-world conditions. We compared our high-level
 784 teleoperation system against a traditional baseline system with joystick control. Results indicate that our
 785 system positively effects task performance and operators comfort during aerial exploration of challenging
 786 indoor environments.

787 In future work we would like to address the limitations of our system (Section 5) and conducted user
 788 study (Section 6.3). Further we would like to evaluate our system in more complicated or even multi-floor
 789 environments, for which abstraction has a potentially larger benefit in terms of overall task performance.

Table 1. User Study Conditions

	JOY Condition	RPG Condition
Type of Control	Traditional Direct	High-Level Supervisory
LOA	1-3	7-10
RPG View	No	Yes
EXO View	Yes	Yes
EGO View	Yes	Yes

790 **Conflict of interest statement**

791 The authors declare that the research was conducted in the absence of any commercial or financial
 792 relationships that could be construed as a potential conflict of interest.

793 **Acknowledgments and funding**

794 The authors wish to thank the collaborators all study participants, the fire brigade Gössendorf, Austria,
 795 and the members of TEDUSAR (Technology and Education for Search and Rescue Robots) group at Graz
 796 University of Technology. This work was funded by FWF grant I1681.

797 **Supplemental Data**

798 We provide a [supplementary video](#) to support the concept of our high-level teleoperation system.

Table 2. Relation between the ALFUS and operating the UAV of our teleoperation system.

ALFUS	Level Definitions	Operating The UAV
[10] Approaching 0% HRI	Highest level of automation, high complexity, all missions, extreme environment	Maximum automation level. Full autonomous exploration of the environment including object detection. The user can still improve task performance by switching to the collaborative levels (e.g., navigation of one preferred portal over the other or inspection of an OOI for verification).
[7-9] Low-level HRI	Collaborative level of automation, high complexity missions, difficult environments	High automation level involving non-mission-critical tasks. Functioning of repetitive low-level tasks is guaranteed (collision-free navigation). The operator can switch to this level, to supervise the system if it fails with complex tasks on highest level. Minimum level that the operator can access in the RPG condition.
[4-6] Medium-level HRI	Medium level of automation and complexity of missions, multi-functional missions, moderate environment	No operator access at this level for RPG condition.
[1-3] High-level HRI	Low level of automation, low level tactical behaviour, simple environments	No operator access at this level for RPG condition. We use that range of levels in the JOY condition.
[0] 100% HRI	Lowest level of automation, full manual remote control by the operator	No operator access at this level for RPG condition.

REFERENCES

- 799 Adams, J. L. (1961). *An investigation of the effects of the time lag due to long transmission distances upon*
800 *remote control. phase i. tracking experiments*. Tech. rep., NATIONAL AERONAUTICS AND SPACE
801 ADMINISTRATION WASHINGTON DC
- 802 Al-Obaidi, M., Mustafa, M., Hasan, W. Z. W., Azis, N. B., Sabry, A., Ang, S., et al. (2019). Efficient
803 charging pad for unmanned aerial vehicle based on direct contact. In *2018 IEEE 5th International*
804 *Conference on Smart Instrumentation, Measurement and Application (ICSIMA)* (IEEE), 1–5
- 805 Alexander, A. D. (1972). Impacts of telemation on modern society. In *On Theory and Practice of Robots*
806 *and Manipulators* (Springer). 121–136
- 807 Alexander III, A. (1972). Survey study of teleoperators. *Robotics, and Remote Systems Technology,*
808 *Remotely Manned Systems Exploration and Operation in Space*, 449–458
- 809 Alexander III, A. D. (1973). A survey study of teleoperators, robotics, and remote systems technology.
- 810 Ambrus, R., Claiici, S., and Wendt, A. (2017). Automatic room segmentation from unstructured 3-d data of
811 indoor environments. *IEEE Robotics and Automation Letters* 2, 749–756
- 812 Angeli, A., Doncieux, S., Meyer, J.-A., and Filliat, D. (2008). Incremental vision-based topological slam.
813 In *Intelligent Robots and Systems, 2008. IROS 2008. IEEE/RSJ International Conference on* (Ieee),
814 1031–1036

- 815 Atherton, J. A. and Goodrich, M. A. (2009). Supporting remote manipulation with an ecological augmented
816 virtuality interface. In *Proc. of the AISB Symposium on New Frontiers in Human-Robot Interaction*,
817 *Edinburgh, Scotland*. 381–394
- 818 Baudisch, P., Good, N., Bellotti, V., and Schraedley, P. (2002). Keeping things in context: a comparative
819 evaluation of focus plus context screens, overviews, and zooming. In *Proceedings of the SIGCHI*
820 *conference on Human factors in computing systems* (ACM), 259–266
- 821 Bhandari, S., Viska, S., Shah, H., Chen, C., Tonini, G., and Kline, S. (2015). Autonomous navigation of a
822 quadrotor in indoor environments for surveillance and reconnaissance. In *AIAA Infotech@ Aerospace*
823 (AIAA SciTech Forum). 0717
- 824 Bormann, R., Jordan, F., Li, W., Hampp, J., and Hägele, M. (2016). Room segmentation: Survey,
825 implementation, and analysis. In *Robotics and Automation (ICRA), 2016 IEEE International Conference*
826 *on* (IEEE), 1019–1026
- 827 Bruemmer, D. J., Dudenhoeffer, D. D., and Marble, J. L. (2002). Dynamic-autonomy for urban search and
828 rescue. In *AAAI mobile robot competition*. 33–37
- 829 Bruemmer, D. J., Few, D. A., Boring, R. L., Marble, J. L., Walton, M. C., and Nielsen, C. W. (2005).
830 Shared understanding for collaborative control. *IEEE Transactions on Systems, Man, and Cybernetics -*
831 *Part A: Systems and Humans* 35, 494–504. doi:10.1109/TSMCA.2005.850599
- 832 Burke, J. L. and Murphy, R. R. (2004). Situation awareness and task performance in robot-assisted technical
833 search: Bujold goes to bridgeport. *citeseer.ist.psu.edu/burke04situation.html*
- 834 Cai, G., Dias, J., and Seneviratne, L. (2014). A survey of small-scale unmanned aerial vehicles: Recent
835 advances and future development trends. *Unmanned Systems* 2, 175–199
- 836 Chellali, R. and Baizid, K. (2011). What maps and what displays for remote situation awareness and rov
837 localization? In *Symposium on Human Interface* (Springer), 364–372
- 838 Chen, T., Ciocarlie, M., Cousins, S., Grice, P. M., Hawkins, K., Hsiao, K., et al. (2013). Robots for
839 humanity: A case study in assistive mobile manipulation. *IEEE Robotics & Automation Magazine*,
840 *Special issue on Assistive Robotics* 20
- 841 Cho, K., Cho, M., and Jeon, J. (2017). Fly a drone safely: Evaluation of an embodied egocentric drone
842 controller interface. *Interacting with computers* 29, 345–354
- 843 Choset, H. and Nagatani, K. (2001). Topological simultaneous localization and mapping (slam): toward
844 exact localization without explicit localization. *IEEE Transactions on robotics and automation* 17,
845 125–137
- 846 Corliss, W. and Johnson, E. (1967). Teleoperators and human augmentation. an aec-nasa technology
847 survey
- 848 Cortellessa, G., Fracasso, F., Sorrentino, A., Orlandini, A., Bernardi, G., Coraci, L., et al. (2018). Robin, a
849 telepresence robot to support older users monitoring and social inclusion: development and evaluation.
850 *Telemedicine and e-Health* 24, 145–154
- 851 Costa, D., Palmieri, G., Palpacelli, M.-C., Panebianco, L., and Scaradozzi, D. (2018). Design of a
852 bio-inspired autonomous underwater robot. *Journal of Intelligent & Robotic Systems* 91, 181–192
- 853 Council, N. R. et al. (1998). *The future of air traffic control: Human operators and automation* (National
854 Academies Press)
- 855 Cui, J., Tosunoglu, S., Roberts, R., Moore, C., and Repperger, D. W. (2003). A review of teleoperation
856 system control. In *Proceedings of the Florida Conference on Recent Advances in Robotics* (Florida
857 Atlantic University Boca Raton, FL), 1–12

- 858 Delmerico, J. A., Baran, D., David, P., Ryde, J., and Corso, J. J. (2013). Ascending stairway modeling from
859 dense depth imagery for traversability analysis. In *2013 IEEE International Conference on Robotics and*
860 *Automation* (IEEE), 2283–2290
- 861 Domahidi, A. and Jerez, J. (2013). Forces pro: code generation for embedded optimization. Homepage.
862 Retrieved November 1, 2018 from <https://www.embotech.com/FORCES-Pro>
- 863 Duan, T., Punpongson, P., Iwai, D., and Sato, K. (2018). Flyinghand: extending the range of haptic
864 feedback on virtual hand using drone-based object recognition. In *SIGGRAPH Asia 2018 Technical*
865 *Briefs* (ACM), 28
- 866 Endsley, M. R. (1999). Level of automation effects on performance, situation awareness and workload in a
867 dynamic control task. *Ergonomics* 42, 462–492
- 868 Endsley, M. R. (2017). From here to autonomy: lessons learned from human–automation research. *Human*
869 *factors* 59, 5–27
- 870 Endsley, M. R. (2018). Level of automation forms a key aspect of autonomy design. *Journal of Cognitive*
871 *Engineering and Decision Making* 12, 29–34
- 872 Erat, O., Isop, W. A., Kalkofen, D., and Schmalstieg, D. (2018). Drone-augmented human vision:
873 Exocentric control for drones exploring hidden areas. *IEEE transactions on visualization and computer*
874 *graphics* 24, 1437–1446
- 875 Espingardeiro, A. (2012). Human performance in telerobotics operations. In *Advanced Materials Research*
876 (Trans Tech Publ), vol. 403, 772–779
- 877 Falanga, D., Kleber, K., Mintchev, S., Floreano, D., and Scaramuzza, D. (2019). The foldable drone: A
878 morphing quadrotor that can squeeze and fly. *IEEE Robotics and Automation Letters* 4, 209–216
- 879 Falanga, D., Mueggler, E., Faessler, M., and Scaramuzza, D. (2017). Aggressive quadrotor flight through
880 narrow gaps with onboard sensing and computing using active vision. In *2017 IEEE International*
881 *Conference on Robotics and Automation (ICRA)* (IEEE), 5774–5781
- 882 Ferland, F., Pomerleau, F., Le Dinh, C. T., and Michaud, F. (2009). Egocentric and exocentric teleoperation
883 interface using real-time, 3d video projection. In *Proceedings of the 4th ACM/IEEE international*
884 *conference on Human robot interaction* (ACM), 37–44
- 885 Ferrell, W. R. (1965). Remote manipulation with transmission delay. *IEEE Transactions on Human Factors*
886 *in Electronics* , 24–32
- 887 Fong, T. and Thorpe, C. (2001). Vehicle teleoperation interfaces. *Autonomous robots* 11, 9–18
- 888 Fong, T., Thorpe, C., and Baur, C. (2003). Multi-robot remote driving with collaborative control. *IEEE*
889 *Transactions on Industrial Electronics* 50, 699–704
- 890 Frohm, J., Lindström, V., Winroth, M., and Stahre, J. (2008). Levels of automation in manufacturing.
891 *Ergonomia*
- 892 Gebhardt, C., Hepp, B., Nægeli, T., Stevšić, S., and Hilliges, O. (2016). Airways: Optimization-based
893 planning of quadrotor trajectories according to high-level user goals. In *Proceedings of the 2016 CHI*
894 *Conference on Human Factors in Computing Systems* (ACM), 2508–2519
- 895 Giernacki, W., Skwierczyński, M., Witwicki, W., Wroński, P., and Koziński, P. (2017). Crazyflie 2.0
896 quadrotor as a platform for research and education in robotics and control engineering. In *2017 22nd*
897 *International Conference on Methods and Models in Automation and Robotics (MMAR)* (IEEE), 37–42
- 898 Goodrich, M. A., McLain, T. W., Anderson, J. D., Sun, J., and Crandall, J. W. (2007). Managing autonomy
899 in robot teams: observations from four experiments. In *Proceedings of the ACM/IEEE international*
900 *conference on Human-robot interaction* (ACM), 25–32

- 901 Hart, S. G. and Staveland, L. E. (1988). Development of nasa-tlx (task load index): Results of empirical and
902 theoretical research. In *Human Mental Workload*, eds. P. A. Hancock and N. Meshkati (North-Holland),
903 vol. 52 of *Advances in Psychology*. 139 – 183. doi:[https://doi.org/10.1016/S0166-4115\(08\)62386-9](https://doi.org/10.1016/S0166-4115(08)62386-9)
- 904 Hedayati, H., Walker, M., and Szafir, D. (2018). Improving collocated robot teleoperation with augmented
905 reality. In *Proceedings of the 2018 ACM/IEEE International Conference on Human-Robot Interaction*
906 (ACM), 78–86
- 907 Held, R. and Durlach, N. (1991). Telepresence, time delay and adaptation. *Pictorial communication in*
908 *virtual and real environments* , 232–246
- 909 Held, R., Efstathiou, A., and Greene, M. (1966). Adaptation to displaced and delayed visual feedback from
910 the hand. *Journal of Experimental Psychology* 72, 887
- 911 HELSINKI, W. D. O. (2013). Ethical principles for medical research involving human subjects. Homepage.
912 Retrieved November 1, 2018 from <https://www.wma.net/policy/current-policies/>
- 913 Henry, P., Krainin, M., Herbst, E., Ren, X., and Fox, D. (2012). Rgb-d mapping: Using kinect-style depth
914 cameras for dense 3d modeling of indoor environments. *The International Journal of Robotics Research*
915 31, 647–663
- 916 Herrmann, R. and Schmidt, L. (2018). Design and evaluation of a natural user interface for piloting an
917 unmanned aerial vehicle. *i-com* 17, 15–24
- 918 Hornung, A., Wurm, K. M., Bennewitz, M., Stachniss, C., and Burgard, W. (2013). Octomap: An efficient
919 probabilistic 3d mapping framework based on octrees. *Auton. Robots* 34, 189–206. doi:10.1007/
920 s10514-012-9321-0
- 921 Huang, A. S., Tellex, S., Bachrach, A., Kollar, T., Roy, D., and Roy, N. (2010). Natural language command
922 of an autonomous micro-air vehicle. In *2010 IEEE/RSJ International Conference on Intelligent Robots*
923 *and Systems* (IEEE), 2663–2669
- 924 Huang, B., Bayazit, D., Ullman, D., Gopalan, N., and Tellex, S. (2019). Flight, camera, action! using
925 natural language and mixed reality to control a drone (ICRA)
- 926 Huang, H.-M., Pavek, K., Albus, J., and Messina, E. (2005a). Autonomy levels for unmanned systems
927 (alfus) framework: An update. In *Unmanned Ground Vehicle Technology VII* (International Society for
928 Optics and Photonics), vol. 5804, 439–449
- 929 Huang, H.-M., Pavek, K., Novak, B., Albus, J., and Messin, E. (2005b). A framework for autonomy
930 levels for unmanned systems (alfus). *Proceedings of the AUVSI's Unmanned Systems North America* ,
931 849–863
- 932 Jha, A. (2016). Unmanned aerial vehicles for military applications. In *Theory, Design, and Applications of*
933 *Unmanned Aerial Vehicles* (CRC Press). 69–124
- 934 Johnson, C. (2018). Topological mapping and navigation in real-world environments
- 935 Johnson, M. and Vera, A. (2019). No ai is an island: The case for teaming intelligence. *AI Magazine* 40,
936 16–28
- 937 Junaid, A. B., Lee, Y., and Kim, Y. (2016). Design and implementation of autonomous wireless charging
938 station for rotary-wing uavs. *Aerospace Science and Technology* 54, 253–266
- 939 Kavraki, L. E. and Latombe, J.-C. (1998). Probabilistic roadmaps for robot path planning
- 940 Kortenkamp, D. M. (1993). *Cognitive maps for mobile robots: A representation for mapping and navigation*.
941 Ph.D. thesis, TRACLabs Inc.
- 942 Kun, D. P., Varga, E. B., and Toth, Z. (2017). Ontology based navigation model of the ilona system. In
943 *2017 IEEE 15th International Symposium on Applied Machine Intelligence and Informatics (SAMI)*
944 (IEEE), 000479–000484

- 945 Kushleyev, A., Mellinger, D., Powers, C., and Kumar, V. (2013). Towards a swarm of agile micro
946 quadrotors. *Autonomous Robots* 35, 287–300
- 947 Kyriatsis, S., Antonopoulos, A., Chanielakis, T., Stefanakis, E., Linardos, C., Tripolitsiotis, A., et al. (2016).
948 Towards autonomous modular uav missions: The detection, geo-location and landing paradigm. *Sensors*
949 16, 1844
- 950 Labbe, M. and Michaud, F. (2013). Appearance-based loop closure detection for online large-scale and
951 long-term operation. *IEEE Transactions on Robotics* 29, 734–745
- 952 Labbe, M. and Michaud, F. (2014). Online Global Loop Closure Detection for Large-Scale Multi-Session
953 Graph-Based SLAM. In *Proceedings of the IEEE/RSJ International Conference on Intelligent Robots*
954 *and Systems*. 2661–2666
- 955 Lan, Z., Shridhar, M., Hsu, D., and Zhao, S. (2017). Xpose: Reinventing user interaction with flying
956 cameras. In *Robotics: Science and Systems*
- 957 Leeper, A. E., Hsiao, K., Ciocarlie, M., Takayama, L., and Gossow, D. (2012). Strategies for human-in-the-
958 loop robotic grasping. In *Proceedings of the Seventh Annual ACM/IEEE International Conference on*
959 *Human-Robot Interaction (ACM), HRI '12*, 1–8. doi:10.1145/2157689.2157691
- 960 Lichiardopol, S. (2007). A survey on teleoperation
- 961 Lin, L. and Goodrich, M. A. (2015). Sliding autonomy for uav path-planning: Adding new dimensions to
962 autonomy management. In *Proceedings of the 2015 International Conference on Autonomous Agents*
963 *and Multiagent Systems (International Foundation for Autonomous Agents and Multiagent Systems)*,
964 1615–1624
- 965 Loianno, G., Brunner, C., McGrath, G., and Kumar, V. (2016). Estimation, control, and planning for
966 aggressive flight with a small quadrotor with a single camera and imu. *IEEE Robotics and Automation*
967 *Letters* 2, 404–411
- 968 MahmoudZadeh, S., Powers, D. M., and Zadeh, R. B. (2018). *Autonomy and Unmanned Vehicles:*
969 *Augmented Reactive Mission and Motion Planning Architecture (Springer)*
- 970 Materna, Z., Španěl, M., Mast, M., Beran, V., Weisshardt, F., Burmester, M., et al. (2017). Teleoperating
971 assistive robots: A novel user interface relying on semi-autonomy and 3d environment mapping. *Journal*
972 *of Robotics and Mechatronics* 29, 381–394
- 973 Monajjemi, M. (2015). Bebop autonomy driver. Homepage. Retrieved November 1, 2018 from https://github.com/AutonomyLab/bebop_autonomy
- 974
- 975 Mostafa, S. A., Ahmad, M. S., and Mustapha, A. (2019). Adjustable autonomy: a systematic literature
976 review. *Artificial Intelligence Review* 51, 149–186
- 977 Mur-Artal, R. and Tardós, J. D. (2017). ORB-SLAM2: an open-source SLAM system for monocular, stereo
978 and RGB-D cameras. *IEEE Transactions on Robotics* 33, 1255–1262. doi:10.1109/TRO.2017.2705103
- 979 Murray, R. M. (2017). *A mathematical introduction to robotic manipulation (CRC press)*
- 980 Muszynski, S., Stückler, J., and Behnke, S. (2012). Adjustable autonomy for mobile teleoperation of
981 personal service robots. In *RO-MAN, 2012 IEEE (IEEE)*, 933–940
- 982 Nagatani, K., Kiribayashi, S., Okada, Y., Otake, K., Yoshida, K., Tadokoro, S., et al. (2013). Emergency
983 response to the nuclear accident at the fukushima daiichi nuclear power plants using mobile rescue
984 robots. *Journal of Field Robotics* 30, 44–63
- 985 Nägeli, T., Alonso-Mora, J., Domahidi, A., Rus, D., and Hilliges, O. (2017a). Real-time motion planning
986 for aerial videography with dynamic obstacle avoidance and viewpoint optimization. *IEEE Robotics and*
987 *Automation Letters* 2, 1696–1703. doi:10.1109/LRA.2017.2665693

- 988 Nägeli, T., Meier, L., Domahidi, A., Alonso-Mora, J., and Hilliges, O. (2017b). Real-time planning for
989 automated multi-view drone cinematography. *ACM Trans. Graph.* 36, 132:1–132:10. doi:10.1145/
990 3072959.3073712
- 991 Nielsen, C. W., Goodrich, M. A., and Ricks, R. W. (2007). Ecological interfaces for improving mobile
992 robot teleoperation. *IEEE Transactions on Robotics* 23, 927–941
- 993 Olson, E. (2011). Apriltag: A robust and flexible visual fiducial system. In *2011 IEEE International
994 Conference on Robotics and Automation*. 3400–3407. doi:10.1109/ICRA.2011.5979561
- 995 Onnasch, L., Wickens, C. D., Li, H., and Manzey, D. (2014). Human performance consequences of stages
996 and levels of automation: An integrated meta-analysis. *Human factors* 56, 476–488
- 997 Optitrack (2019). Flex 13. Homepage. Retrieved March 1, 2019 from [www.optitrack.com/
998 products/flex-13/](http://www.optitrack.com/products/flex-13/)
- 999 Papachristos, C., Khattak, S., and Alexis, K. (2017). Uncertainty-aware receding horizon exploration
1000 and mapping using aerial robots. In *2017 IEEE International Conference on Robotics and Automation
1001 (ICRA) (IEEE)*, 4568–4575
- 1002 Parasuraman, R., Sheridan, T. B., and Wickens, C. D. (2000). A model for types and levels of human
1003 interaction with automation. *IEEE Transactions on systems, man, and cybernetics-Part A: Systems and
1004 Humans* 30, 286–297
- 1005 Parrot (2015). Parrot bebop 2. Homepage. Retrieved November 1, 2018 from [https://www.parrot.
1006 com/us/drones/parrot-bebop-2](https://www.parrot.com/us/drones/parrot-bebop-2)
- 1007 Paterson, J., Han, J., Cheng, T., Laker, P., McPherson, D., Menke, J., et al. (2019). Improving
1008 usability, efficiency, and safety of uav path planning through a virtual reality interface. *arXiv preprint
1009 arXiv:1904.08593*
- 1010 Patra, R. K., Nedeveschi, S., Surana, S., Sheth, A., Subramanian, L., and Brewer, E. A. (2007). Wildnet:
1011 Design and implementation of high performance wifi based long distance networks. In *NSDI*. vol. 1, 1
- 1012 Rakita, D., Mutlu, B., and Gleicher, M. (2018). An autonomous dynamic camera method for effective
1013 remote teleoperation. In *Proceedings of the 2018 ACM/IEEE International Conference on Human-Robot
1014 Interaction (ACM)*, 325–333
- 1015 Razor (2015). Orbweaver. Homepage. Retrieved March 1, 2019 from [https://www.razer.com/
1016 gaming-keyboards-keypads/razer-orbweaver-chroma](https://www.razer.com/gaming-keyboards-keypads/razer-orbweaver-chroma)
- 1017 Redmon, J., Divvala, S., Girshick, R., and Farhadi, A. (2016). You only look once: Unified, real-time
1018 object detection. In *Proceedings of the IEEE conference on computer vision and pattern recognition*.
1019 779–788
- 1020 Reese, H. (2016). Autonomous driving levels 0 to 5: Understanding the differences.
1021 Homepage. Retrieved November 1, 2018 from [https://www.techrepublic.com/article/
1022 autonomous-driving-levels-0-to-5-understanding-the-differences/](https://www.techrepublic.com/article/autonomous-driving-levels-0-to-5-understanding-the-differences/)
- 1023 Richtsfeld, A., Morwald, T., Prankl, J., Zillich, M., and Vincze, M. (2012). Segmentation of unknown
1024 objects in indoor environments. In *2012 IEEE/RSJ International Conference on Intelligent Robots and
1025 Systems*. 4791–4796. doi:10.1109/IROS.2012.6385661
- 1026 Riestock, M., Engelhardt, F., Zug, S., and Hochgeschwender, N. (2017a). Exploring gridmap-based
1027 interfaces for the remote control of uavs under bandwidth limitations. In *Proceedings of the Companion
1028 of the 2017 ACM/IEEE International Conference on Human-Robot Interaction (ACM)*, 263–264
- 1029 Riestock, M., Engelhardt, F., Zug, S., and Hochgeschwender, N. (2017b). User study on remotely controlled
1030 uavs with focus on interfaces and data link quality. In *2017 IEEE/RSJ International Conference on
1031 Intelligent Robots and Systems (IROS) (IEEE)*, 3394–3400

- 1032 Robotics, A. (2019). Evo drone. Homepage. Retrieved March 1, 2019 from [https://autel drones .](https://autel drones.com/products/evo)
1033 [com/products/evo](https://autel drones.com/products/evo)
- 1034 Rognon, C., Mintchev, S., Dell’Agnola, F., Cherpillod, A., Atienza, D., and Floreano, D. (2018). Flyjacket:
1035 An upper body soft exoskeleton for immersive drone control. *IEEE Robotics and Automation Letters* 3,
1036 2362–2369
- 1037 Saakes, D., Choudhary, V., Sakamoto, D., Inami, M., and Lgarashi, T. (2013). A teleoperating interface for
1038 ground vehicles using autonomous flying cameras. In *2013 23rd International Conference on Artificial*
1039 *Reality and Telexistence (ICAT) (IEEE)*, 13–19
- 1040 SAE (2014). Taxonomy and definitions for terms related to on-road motor vehicle automated driving
1041 systems. Homepage. Retrieved November 1, 2018 from [https://saemobilus.sae.org/](https://saemobilus.sae.org/content/j3016_201401)
1042 [content/j3016_201401](https://saemobilus.sae.org/content/j3016_201401)
- 1043 Sanders, B., Vincenzi, D., Holley, S., and Shen, Y. (2018). Traditional vs gesture based uav control. In
1044 *International Conference on Applied Human Factors and Ergonomics (Springer)*, 15–23
- 1045 Sanket, N. J., Singh, C. D., Ganguly, K., Fermüller, C., and Aloimonos, Y. (2018). Gapflyt: Active vision
1046 based minimalist structure-less gap detection for quadrotor flight. *IEEE Robotics and Automation Letters*
1047 3, 2799–2806
- 1048 Save, L., Feuerberg, B., and Avia, E. (2012). Designing human-automation interaction: a new level of
1049 automation taxonomy. *Proc. Human Factors of Systems and Technology 2012*
- 1050 Scalea, J. R., Restaino, S., Scassero, M., Bartlett, S. T., and Wereley, N. (2019). The final frontier?
1051 exploring organ transportation by drone. *American Journal of Transplantation* 19, 962–964
- 1052 Schröter, D., Beetz, M., and Radig, B. (2003). Rg mapping: Building object-oriented representations of
1053 structured human environments. In *6th Open Russian–German Workshop on Pattern Recognition and*
1054 *Image Understanding (OGRW)*
- 1055 Seo, S. H., Rea, D. J., Wiebe, J., and Young, J. E. (2017). Monocle: Interactive detail-in-context using two
1056 pan-and-tilt cameras to improve teleoperation effectiveness. In *2017 26th IEEE International Symposium*
1057 *on Robot and Human Interactive Communication (RO-MAN) (IEEE)*, 962–967
- 1058 Sheridan, T. B. (1992). *Telerobotics, automation, and human supervisory control* (MIT press)
- 1059 Sheridan, T. B. (1993). Space teleoperation through time delay: Review and prognosis. *IEEE Transactions*
1060 *on robotics and Automation* 9, 592–606
- 1061 Sheridan, T. B. and Verplank, W. L. (1978). *Human and computer control of undersea teleoperators*. Tech.
1062 rep., Massachusetts Inst of Tech Cambridge Man-Machine Systems Lab
- 1063 Silvagni, M., Tonoli, A., Zenerino, E., and Chiaberge, M. (2019). Multipurpose uav for search and rescue
1064 operations in mountain avalanche events mario silvagni1, andrea tonoli1, enrico zenerino1, marcello
1065 chiaberge2
- 1066 Stepanova, E. R., von der Heyde, M., Kitson, A., Schiphorst, T., and Riecke, B. E. (2017). Gathering and
1067 applying guidelines for mobile robot design for urban search and rescue application. In *International*
1068 *Conference on Human-Computer Interaction (Springer)*, 562–581
- 1069 Stubbs, K., Hinds, P. J., and Wettergreen, D. (2007). Autonomy and common ground in human-robot
1070 interaction: A field study. *IEEE Intelligent Systems* 22
- 1071 Szafir, D., Mutlu, B., and Fong, T. (2017). Designing planning and control interfaces to support user
1072 collaboration with flying robots. *The International Journal of Robotics Research* 36, 514–542
- 1073 Technology, A. (2014). Bomb disposal robots - evolution and revolution. Homepage.
1074 Retrieved March 1, 2019 from [https://www.army-technology.com/features/](https://www.army-technology.com/features/featurebomb-disposal-robots-evolution-and-revolution/)
1075 [featurebomb-disposal-robots-evolution-and-revolution/](https://www.army-technology.com/features/featurebomb-disposal-robots-evolution-and-revolution/)

- 1076 Thomason, J., Ratsamee, P., Kiyokawa, K., Kriangkamol, P., Orlosky, J., Mashita, T., et al. (2017).
1077 Adaptive view management for drone teleoperation in complex 3d structures. In *Proceedings of the*
1078 *22nd International Conference on Intelligent User Interfaces (ACM)*, 419–426
- 1079 Thomason, J., Ratsamee, P., Orlosky, J., Kiyokawa, K., Mashita, T., Uranishi, Y., et al. (2019). A
1080 comparison of adaptive view techniques for exploratory 3d drone teleoperation. *ACM Transactions on*
1081 *Interactive Intelligent Systems (TiIS)* 9, 17
- 1082 Tripicchio, P., Satler, M., Dabisias, G., Ruffaldi, E., and Avizzano, C. A. (2015). Towards smart farming
1083 and sustainable agriculture with drones. In *2015 International Conference on Intelligent Environments*
1084 (IEEE), 140–143
- 1085 Umari, H. and Mukhopadhyay, S. (2017). Autonomous robotic exploration based on multiple rapidly-
1086 exploring randomized trees. In *2017 IEEE/RSJ International Conference on Intelligent Robots and*
1087 *Systems (IROS)*. 1396–1402. doi:10.1109/IROS.2017.8202319
- 1088 Valero-Gomez, A., De La Puente, P., and Hernando, M. (2011). Impact of two adjustable-autonomy models
1089 on the scalability of single-human/multiple-robot teams for exploration missions. *Human factors* 53,
1090 703–716
- 1091 Valner, R., Kruusamäe, K., and Pryor, M. (2018). Temoto: Intuitive multi-range telerobotic system with
1092 natural gestural and verbal instruction interface. *Robotics* 7, 9
- 1093 Vasudevan, S., Gächter, S., Nguyen, V., and Siegwart, R. (2007). Cognitive maps for mobile robots-an
1094 object based approach. *Robot. Auton. Syst.* 55, 359–371. doi:10.1016/j.robot.2006.12.008
- 1095 Vertut, J. and Coiffet, P. (1986). Teleoperations and robotics: Evolution and development, “robot technology,”
1096 vol. 3a
- 1097 Walker, M. E., Hedayati, H., and Szafir, D. (2019). Robot teleoperation with augmented reality virtual
1098 surrogates. In *2019 14th ACM/IEEE International Conference on Human-Robot Interaction (HRI)*
1099 (IEEE), 202–210
- 1100 Wang, L., Zhao, L., Huo, G., Li, R., Hou, Z., Luo, P., et al. (2018). Visual semantic navigation based on
1101 deep learning for indoor mobile robots. *Complexity* 2018
- 1102 Weiss, S., Scaramuzza, D., and Siegwart, R. (2011). Monocular-slam-based navigation for autonomous
1103 micro helicopters in gps-denied environments. *Journal of Field Robotics* 28, 854–874
- 1104 Wu, Y., Du, X., Duivenvoorden, R., and Kelly, J. (2018). Hummingbird: An open-source dual-rotor
1105 tail-sitter platform for research and education. *arXiv preprint arXiv:1810.03196*
- 1106 Yanco, H. A., Drury, J. L., and Scholtz, J. (2004). Beyond usability evaluation: Analysis of human-robot
1107 interaction at a major robotics competition. *Human-Computer Interaction* 19, 117–149
- 1108 Yang, L. and Worboys, M. (2015). Generation of navigation graphs for indoor space. *International Journal*
1109 *of Geographical Information Science* 29, 1737–1756
- 1110 Yu, M., Lin, Y., Schmidt, D., Wang, X., and Wang, Y. (2014). Human-robot interaction based on gaze
1111 gestures for the drone teleoperation. *Journal of Eye Movement Research* 7, 1–14
- 1112 Yu, Y., Wang, X., Zhong, Z., and Zhang, Y. (2017). Ros-based uav control using hand gesture recognition.
1113 In *2017 29th Chinese Control And Decision Conference (CCDC)* (IEEE), 6795–6799
- 1114 Yuan, L., Reardon, C., Warnell, G., and Loianno, G. (2019). Human gaze-driven spatial tasking of an
1115 autonomous mav. *IEEE Robotics and Automation Letters* 4, 1343–1350
- 1116 Zhang, Q., Zhao, W., Chu, S., Wang, L., Fu, J., Yang, J., et al. (2018). Research progress of nuclear
1117 emergency response robot. In *IOP Conference Series: Materials Science and Engineering* (IOP
1118 Publishing), vol. 452, 042102